



Calhoun: The NPS Institutional Archive
DSpace Repository

Theses and Dissertations

1. Thesis and Dissertation Collection, all items

2020

**HYDROGEN ENHANCED ATOMIC TRANSPORT:
CREATING HARD TITANIUM/TITANIUM
HYDRIDE BROWN BODIES AT AMBIENT
PRESSURE AND TEMPERATURE GREATER
THAN 650 DEGREES CENTIGRADE**

Janssen, Anthony J.

Monterey, CA; Naval Postgraduate School

<http://hdl.handle.net/10945/65553>

This publication is a work of the U.S. Government as defined in Title 17, United States Code, Section 101. Copyright protection is not available for this work in the United States.

Downloaded from NPS Archive: Calhoun



Calhoun is the Naval Postgraduate School's public access digital repository for research materials and institutional publications created by the NPS community. Calhoun is named for Professor of Mathematics Guy K. Calhoun, NPS's first appointed -- and published -- scholarly author.

Dudley Knox Library / Naval Postgraduate School
411 Dyer Road / 1 University Circle
Monterey, California USA 93943

<http://www.nps.edu/library>



NAVAL POSTGRADUATE SCHOOL

MONTEREY, CALIFORNIA

THESIS

**HYDROGEN ENHANCED ATOMIC TRANSPORT: CREATING
HARD TITANIUM/TITANIUM HYDRIDE BROWN BODIES AT
AMBIENT PRESSURE AND TEMPERATURE GREATER
THAN 650 DEGREES CENTIGRADE**

by

Anthony J. Janssen

June 2020

Thesis Advisor:

Jonathan Phillips

Co-Advisor:

Claudia C. Luhrs

Approved for public release. Distribution is unlimited.

THIS PAGE INTENTIONALLY LEFT BLANK

REPORT DOCUMENTATION PAGE			<i>Form Approved OMB No. 0704-0188</i>	
Public reporting burden for this collection of information is estimated to average 1 hour per response, including the time for reviewing instruction, searching existing data sources, gathering and maintaining the data needed, and completing and reviewing the collection of information. Send comments regarding this burden estimate or any other aspect of this collection of information, including suggestions for reducing this burden, to Washington headquarters Services, Directorate for Information Operations and Reports, 1215 Jefferson Davis Highway, Suite 1204, Arlington, VA 22202-4302, and to the Office of Management and Budget, Paperwork Reduction Project (0704-0188) Washington, DC 20503.				
1. AGENCY USE ONLY (Leave blank)		2. REPORT DATE June 2020		3. REPORT TYPE AND DATES COVERED Master's thesis
4. TITLE AND SUBTITLE HYDROGEN ENHANCED ATOMIC TRANSPORT: CREATING HARD TITANIUM/TITANIUM HYDRIDE BROWN BODIES AT AMBIENT PRESSURE AND TEMPERATURE GREATER THAN 650 DEGREES CENTIGRADE			5. FUNDING NUMBERS	
6. AUTHOR(S) Anthony J. Janssen				
7. PERFORMING ORGANIZATION NAME(S) AND ADDRESS(ES) Naval Postgraduate School Monterey, CA 93943-5000			8. PERFORMING ORGANIZATION REPORT NUMBER	
9. SPONSORING / MONITORING AGENCY NAME(S) AND ADDRESS(ES) N/A			10. SPONSORING / MONITORING AGENCY REPORT NUMBER	
11. SUPPLEMENTARY NOTES The views expressed in this thesis are those of the author and do not reflect the official policy or position of the Department of Defense or the U.S. Government.				
12a. DISTRIBUTION / AVAILABILITY STATEMENT Approved for public release. Distribution is unlimited.			12b. DISTRIBUTION CODE A	
13. ABSTRACT (maximum 200 words) This thesis introduces a simple, low-temperature method called Hydrogen Enhanced Atomic Transport (HEAT) for creating metallic bonded brown bodies on the order of 40% bulk density in molds of designed shape from titanium (Ti) metal particles. In this initial study, 40 µm Ti particles were poured into graphite molds and heated for four hours to temperatures greater than 650 °C in a flowing ambient pressure gas mixture containing some hydrogen, which led to brown body formation that closely mimicked the mold shape. The brown bodies were shown to be hard, and consisted of primarily Ti metal and some titanium hydride. It is postulated that hydrogen is key to the sintering mechanism: it enables the formation of short-lived volatile titanium hydride species that lead to sintering via an Ostwald Ripening mechanism. Data consistent with this postulate includes finding that brown bodies formed with hydrogen present (HEAT process) had mechanical properties like metal, such that they plastically deformed at high pressure (ca. 5000 atm). In contrast, brown bodies made in identical conditions but without hydrogen were brittle and broke into micron-scale particles under pressure. HEAT appears to have advantages relative to existing titanium metal additive manufacturing methods, such as particle injection molding, which requires many more steps, particularly debonding, and other methods, such as laser sintering, which are slower and require expensive hardware and expert operation.				
14. SUBJECT TERMS Reduction Expansion Synthesis-Sintered Metal, RES-SM, titanium, titanium hydride, Navy, low temperature, HEAT, Hydrogen Enhanced Atomic Transport, cellular metal foams			15. NUMBER OF PAGES 79	
			16. PRICE CODE	
17. SECURITY CLASSIFICATION OF REPORT Unclassified	18. SECURITY CLASSIFICATION OF THIS PAGE Unclassified	19. SECURITY CLASSIFICATION OF ABSTRACT Unclassified	20. LIMITATION OF ABSTRACT UU	

THIS PAGE INTENTIONALLY LEFT BLANK

Approved for public release. Distribution is unlimited.

**HYDROGEN ENHANCED ATOMIC TRANSPORT: CREATING HARD
TITANIUM/TITANIUM HYDRIDE BROWN BODIES AT AMBIENT
PRESSURE AND TEMPERATURE GREATER THAN 650 DEGREES
CENTIGRADE**

Anthony J. Janssen
Ensign, United States Navy
BS, United States Naval Academy, 2019

Submitted in partial fulfillment of the
requirements for the degree of

**MASTER OF SCIENCE IN ENGINEERING SCIENCE
(AEROSPACE ENGINEERING)**

from the

**NAVAL POSTGRADUATE SCHOOL
June 2020**

Approved by: Jonathan Phillips
Advisor

Claudia C. Luhrs
Co-Advisor

Garth V. Hobson
Chair, Department of Mechanical and Aerospace Engineering

THIS PAGE INTENTIONALLY LEFT BLANK

ABSTRACT

This thesis introduces a simple, low-temperature method called Hydrogen Enhanced Atomic Transport (HEAT) for creating metallic bonded brown bodies on the order of 40% bulk density in molds of designed shape from titanium (Ti) metal particles. In this initial study, 40 μm Ti particles were poured into graphite molds and heated for four hours to temperatures greater than 650 °C in a flowing ambient pressure gas mixture containing some hydrogen, which led to brown body formation that closely mimicked the mold shape. The brown bodies were shown to be hard, and consisted of primarily Ti metal and some titanium hydride. It is postulated that hydrogen is key to the sintering mechanism: it enables the formation of short-lived volatile titanium hydride species that lead to sintering via an Ostwald Ripening mechanism. Data consistent with this postulate includes finding that brown bodies formed with hydrogen present (HEAT process) had mechanical properties like metal, such that they plastically deformed at high pressure (ca. 5000 atm). In contrast, brown bodies made in identical conditions but without hydrogen were brittle and broke into micron-scale particles under pressure. HEAT appears to have advantages relative to existing titanium metal additive manufacturing methods, such as particle injection molding, which requires many more steps, particularly debonding, and other methods, such as laser sintering, which are slower and require expensive hardware and expert operation.

THIS PAGE INTENTIONALLY LEFT BLANK

TABLE OF CONTENTS

I.	INTRODUCTION.....	1
II.	PURE TITANIUM.....	3
A.	INTRODUCTION.....	3
B.	EXPERIMENTAL METHODS	6
1.	Precursors.....	7
2.	Sample Mold.....	9
3.	Sample in Furnace—Firing.....	11
4.	Materials Characterization	12
C.	RESULTS	24
1.	Visual/Macro Observations.....	25
2.	TGA	26
3.	XRD	28
4.	Ohaus Density Analysis	30
5.	Scanning Electron Microscope	31
6.	Instron Compression	33
III.	THE CONTRIBUTIONS OF TITANIUM HYDRIDE.....	37
A.	INTRODUCTION.....	37
B.	BACKGROUND	38
C.	EXPERIMENTAL METHODS	40
1.	Precursors.....	40
2.	Sample Mold.....	42
3.	Furnace	43
4.	Materials characterization	43
D.	RESULTS	43
1.	Visual/Macro Observations.....	43
2.	TGA	44
3.	SEM.....	44
IV.	DISCUSSION	47
V.	FUTURE TESTING	51
VI.	CONCLUSION	53
	LIST OF REFERENCES	55
	INITIAL DISTRIBUTION LIST	61

THIS PAGE INTENTIONALLY LEFT BLANK

LIST OF FIGURES

Figure 1.	Sigma Aldrich – Ti and TiH ₂ metal powder.....	7
Figure 2.	Sample mold: Top view	9
Figure 3.	Sample mold: Side view	10
Figure 4.	Lindburgh-Blue M 24” Single Zone Furnace use for all samples	11
Figure 5.	Thermal Gravimetric Analyzer	13
Figure 6.	Rigaku Miniflex 600 X-ray Diffractometer	14
Figure 7.	Mirrored sample carriage	15
Figure 8.	Ziess Neon 40 FESEM and EDS. Source: [12].	17
Figure 9.	Specimen and electron interaction. Source: [31].	18
Figure 10.	Ohaus density test	19
Figure 11.	Vacuum chamber used for density analysis (L. pump, R. chamber)	20
Figure 12.	Fisher Scientific (FS110) Digital Ultrasonic Cleaning Bath	21
Figure 13.	Side-view of Instron.....	22
Figure 14.	Front-view of Instron	23
Figure 15.	Stability after mild shaking	26
Figure 16.	TGA results.....	27
Figure 17.	XRD analysis of raw material (A, D) and solid samples (B, E, C, F)	29
Figure 18.	SEM images of samples prepared with and without hydrogen.....	32
Figure 19.	Features dependent on hydrogen flow	33
Figure 20.	Compression distortion	34
Figure 21.	Comparing crushed samples	35
Figure 22.	Density as a function of applied pressure at ambient temperature. Adapted from [35].....	36

Figure 23.	Sigma Aldrich – Titanium (II) hydride, 325 mesh, 98% metal basis	41
Figure 24.	Titanium Hydride sample	44
Figure 25.	SEM images prepared of titanium hydride in forming gas to a control sample prepared in argon.....	45
Figure 26.	HEAT process leads to adjacent particles joining	46

LIST OF TABLES

Table 1.	Primary test description—Pure titanium.....	8
Table 2.	XRD measurement conditions	16
Table 3.	Parameters for XRD run	26
Table 4.	Density of samples fired in forming gas—Not compressed	31
Table 5.	Testing parameters for all test using titanium hydride.....	42

THIS PAGE INTENTIONALLY LEFT BLANK

LIST OF ACRONYMS AND ABBREVIATIONS

BB	Traditional Brown Body
EDS	Energy Dispersive Spectroscopy
HEAT	Hydrogen Enhanced Atomic Transport
HIP	Hot Isostatic Pressing
MAT	Mobile Atomic Titanium
MIM	Metal Powder Injection Molding
NPS	Naval Postgraduate School
OR	Ostwald Ripening
RES	Reduction Expansion Synthesis
RES-SM	Reduction Expansion Synthesis Sintered Metal
SBB	Strong Brown Body
SE	Secondary Electrons
SEM	Scanning Electron Microscope
UHP	Ultra-High Purity
WBB	Weak Brown Bodies
XRD	X-ray Diffraction

THIS PAGE INTENTIONALLY LEFT BLANK

ACKNOWLEDGMENTS

I would like to give my deepest thanks to my supreme leader, Professor Phillips. He guided me through my studies with grace and skill. I was his apprentice and felt much like Anakin Skywalker with Dr. Phillips being my Obi-Wan (with the exception that I did not turn to the dark side). I would also like to specifically thank Dr. Park, Dr. Luhrs, and CDR Earp for being amazing resources throughout my year at NPS. From day one, I was welcomed with open arms into the department. The kindness and knowledge shared was immeasurable.

Professor Ansell, I would also like to thank you for dealing with my antics. I will deeply miss walking by your office for no other reason but to distract you, wave, and leave. I hope I can find another student to replace me in being equally as annoying, but I doubt I will be successful in that endeavor. Also, if you thought that this is where I would forgive you for going to Hawaii without me, you would be wrong! I am taking that to the grave!

To the memories that can only be made in Monterey, California.

—Tony

THIS PAGE INTENTIONALLY LEFT BLANK

I. INTRODUCTION

The objective of this research was to explore a novel method for low temperature sintering of titanium. The outcome of this objective was a new method of titanium additive manufacturing, Hydrogen Enhanced Atomic Transport (HEAT). Although the HEAT process was inspired by Reduction Expansion Synthesis (RES), it is based on a novel chemistry [1–12]. RES utilizes the reducing agents, produced by exposing urea to a high temperature, to reduce a metal oxide and produce a fully sintered metal body [2–5,9–12]. This reduction of the metal oxide promotes sintering of adjacent metal particles via Ostwald Ripening (OR) [13,14]. RES was particularly successful for Ni, Fe, and Cr, but due to variable stability of metal oxides in the presence of reducing agents, titanium was not a metal that could be utilized with RES.

Titania (TiO_2), like many other metal oxides, is too stable for reduction by radicals, which is the key mechanism by which low temperature sintering takes place via RES. Titanium itself was settled upon due to its desirable mechanical characteristics, such as biocompatibility, low reactivity, low weight, and high strength. These qualities lend themselves to a wide array of applications in the medical, military, and automotive industries.

With the objective of finding a low-temperature sintering mechanism for titanium in mind, research questions were also presented. If low temperature sintering cannot take place via reduction by radicals, what other means could be used to facilitate sintering of titanium? What is the lowest temperature that a mechanically stable solid can be generated? What are the applications for a porous titanium sample and what would be required to generate a fully sintered titanium part? Hydrogen Enhanced Atomic Transport (HEAT), a novel method for producing low temperature titanium brown bodies, was the byproduct of these questions and the research presented in this paper.

THIS PAGE INTENTIONALLY LEFT BLANK

II. PURE TITANIUM

In this paper, an analysis of the sintering of titanium and titanium hydride powders to form solid bodies with and without hydrogen is presented. Chapter one explores pure titanium.

A. INTRODUCTION

This paper describes a novel method for additive manufacture of brown titanium parts from titanium particles, a method mechanistically related to Reduction Expansion Synthesis-Sintered Metal (RES-SM) but based on a novel chemistry. This process, Hydrogen Enhanced Atomic Transport (HEAT), is simple in practice: at elevated temperatures and ambient pressure a gas mixture containing hydrogen and inert gas is flowed over a titanium particle bed contained in an inert (e.g., graphitic) mold. At relatively low temperatures ($<650\text{ }^{\circ}\text{C}$) and with sufficient time (ca. 4 hours) brown bodies will form. These solid bodies will be identical in shape to the mold. These brown bodies are composed of two phases: titanium and titanium hydride.

All observations fully support the model that the successful production of brown titanium/titanium hydride metal bodies using HEAT occurs via this mechanism: titanium hydride, (TiH_2) readily forms in a hydrogen containing environment as predicted by thermodynamic phase diagrams. It is anticipated that, as per kinetic theory, the titanium hydride concentration reaches steady state due to a balance between formation and the decomposition process. It is postulated that this species has a relatively high vapor pressure at elevated temperatures, leading to “transport” of this species in molecular form within the bed. Subsequent decomposition leads to titanium deposition/transport.

The precise nature of the titanium hydride transport is not known but could be via a combination of surface and gas diffusion. Transport of material within a particle bed at the atomic/molecular scale is well-known to lead to Ostwald Ripening (OR). Specifically, OR leads to large particles grown at the expense of small particles [13,14]. A similar “metal radical” model is used to explain the growth of large metal particles in the gas phase during catalytic etching [15] as well as the enhanced rates of particle growth in supported catalysts

under reaction conditions [16]. In the case of the titanium particles treated in this study, the process is postulated to lead to growth in the average particle size via chemical bonds forming between particles. The ultimate product is a titanium brown body.

The development of the HEAT process represents a further evolution of Reduction Expansion Synthesis (RES) [1–12], a set of technologies based on a novel “reduction” chemistry introduced by our team. The novel RES chemistry in all cases starts with a primary step: thermal decomposition of solids, such as urea, under inert gas. This primary step chemistry creates volatile “reducing” radicals that can be harnessed to create a wide range of products based on designed secondary reactions. Novel processes developed on the basis of the RES concept include the batch generation of sub-micron metal and metal alloy particles [3–5], metal thin film formation [9,10], metal part formation from mixtures of metal and metal oxide particles [2,11,12], graphene from graphite oxide [6], and stable tin/carbon anodes for batteries [7].

In all “metal” variants of RES [2–5,9–12] the key to the secondary step is the reaction between reducing radicals and metal oxide species. It is postulated that the radicals interact with oxygen atoms in metal oxides to create products such as CO_2 and H_2O that subsequently leave the process reactor as a gas. The heavy metal atoms/metallic clusters produced via the removal of oxygen are not volatile and do not leave the reactor. Instead, based on proper arrangement of materials within the bed, these species migrate, as per the OR mechanism, leading to metal particle growth and sintering. The process has been demonstrated to lead to growth and sintering of metal, specifically Ni, Fe and Cr, objects from beds consisting originally of particles of metal and oxide. This leads to the creation of designed solid metal objects, thus this type of RES, RES-Sintered Metals (RES-SM) is a form of metal additive manufacturing.

The inherent chemical limitations of the RES-SM method to only a few materials led to the invention of HEAT. Indeed, RES will not work for metal oxides, including titania, which are too stable for reduction by radicals even at 1000 °C yet, the motivation for finding an RES-like process for metal additive manufacturing of titanium parts is clear. Titanium and titanium alloys are widely used in aerospace, automotive, chemical and biomedical industry because of its great strength, low weight and excellent corrosion

resistance [17–19]. Also, titanium is very expensive, thus “subtractive” manufacturing involves a significant cost, because cut metal must be reprocessed. Thus, HEAT was invented to create a new primary step for titanium sintering and/or a novel method for manufacturing cellular titanium foams (primarily used in the biomedical industry). The generation of mobile, but short-lived titanium hydride species is postulated to be the primary step in HEAT. The subsequent HEAT secondary steps lead to OR, very similar to that in RES.

In HEAT and RES-SM, the dominant means of metal transport is hypothesized to be via atomic metal species, which leads, via OR, to chemical bonding and sintering. HEAT, like RES-SM, creates brown bodies at ambient pressure and at a temperature far below the melting temperature.

The outcome of this study is significant as it suggests a way forward to create brown, designed, titanium and titanium alloy metal parts more quickly and with less investment than any other commercial process for creating metal parts of designed shape from particles. This includes laser particle bed sintering and related metal additive manufacturing technologies and metal powder injection molding (MIM). In practice, MIM and RES are potentially competitors in the low cost, high throughput metal form parts from particles market. Additive manufacturing is far more expensive, slower, but a more precise and flexible technology.

Prior to the present study, the only method for titanium part creation was the MIM process [20,21], as RES cannot be used to create titanium brown bodies. Many variations on the MIM process have been studied, including the use of titanium hydride as a “sintering aid” [22–25]; however, in all cases both high temperature ($> 1000\text{ }^{\circ}\text{C}$) and high pressure, more than 1000 atmospheres are required to create a brown body. Also, the MIM process is multi-step:

1. A green body containing a binder (wax) is formed by high pressure injection into a metal mold followed by moderate heating.
2. The binder is removed in a slow heating step (debinding).

3. The metal is sintered at high temperature to create a titanium brown body.

An advantage to the HEAT process, like the advantages of RES, is that neither high temperature nor pressure is required to create a titanium brown body. Only one step is required: Heat (>650 °C) titanium particles in a mold at ambient pressure in a gas containing hydrogen for a few hours.

B. EXPERIMENTAL METHODS

Much of the experimental method described parallels that which was established by Wilson Rydalch in 2019 during his research [12]. In the research by Rydalch, nickel sintering was achieved through the Reduction Expansion Synthesis (RES) process. For nickel, sintering was achieved via necking between adjacent metal particles following the reduction of metal oxide particles. The reduction of the metal oxide particles produced mobile metal atoms that would diffuse and join existing metal crystal structures. The ultimate achievement of this process is the ability to create a solid object at temperatures much lower than what is needed for traditional sintering [12]. Unlike previous experiments, though, a novel method for titanium sintering was explored.

Inspired by the Reduction Expansion Synthesis-Sinter Metal process, Hydrogen Enhanced Atomic Transport employs a similar protocol, but two protocol changes lead to a unique chemistry/sintering mechanism. First, only pure metal particles are placed in a mold. In RES-SM both metal and metal oxide particles are required. Second, the metal powder is exposed to a gas mixture at an elevated temperature (>650 °C), composed primarily of inert gas (argon), but also containing a low concentration of active hydrogen. In RES-SM the sample is exposed to an inert gas at an elevated temperature (>800 °C), typically argon or nitrogen. It is postulated these changes lead to a distinctly different metal transport/sintering process. In HEAT it is postulated sintering occurs via volatilized titanium hydride, whereas in RES-SM the transport species are postulated to be metal atoms, or clusters, formed when oxygen is removed from the oxide particles in the mold.

Characterization of the resulting metal “brown bodies” was performed using Thermal Gravimetric Analysis (TGA), X-Ray Diffraction (XRD), Scanning Electron Microscopy (SEM), Ohaus Density analysis, and Instron compressive testing.

1. Precursors

In most cases the precursor material was titanium powder (Sigma Aldrich – Ti powder, 325 mesh, 99.9% metal basis), average particle size (less than 44 microns). The weight of the input titanium powder was in all cases 0.5 +/- 20% gms. In several cases mixtures of titanium and titanium hydride (Sigma Aldrich – Titanium [II] hydride, 325 mesh, 98% metal basis) were employed. Any test that employed a mixture of titanium and titanium hydride is discussed in Chapter II. Images of the powders used can be seen in Figure 1.



Figure 1. Sigma Aldrich – Ti and TiH₂ metal powder

In all cases reported here in (Table 1) the precursor material was exclusively pure titanium powder (Sigma Aldrich – Ti powder, 325 mesh, 99.9% metal basis), which has an average particle size of approximately 40 microns, as mentioned. These tests formed the backbone of research conducted. Following the generation of these samples, many of them were compressed at various pressures. Samples that withstood compression at or near 5000 atmospheres were declared strong brown bodies (SBB). Samples that did not meet this specification were considered weak brown bodies (WBB). All of the WBB were control

samples that were formed in identical conditions to that of those produced via the HEAT process but in the absence of hydrogen flow during firing.

Table 1. Primary test description—Pure titanium

Test	Firing Temp (°C)	Flow	Key Visual Observations—Raw	Key Visual Observations—Post-compression
1	650	Ar/H	Solid	Metallic Bonded Solid/modest shape change/SBB
2	650	Ar	Powder	-
3	650	Ar	Powder	-
4	650	Ar/H	Solid	Metallic Bonded Solid/modest shape change (5000 Atm)/SBB
5	550	Ar/H	Unstable solid	-
6	750	Ar/H	Solid	Metallic Bonded Solid/modest shape change (5000 Atm)/SBB
7	750	Ar	Powder	Only powder after compression (5000 Atm)
8	850	Ar/H	Solid	Metallic Bonded Solid/modest shape change (5000 Atm)/SBB
9	950	Ar/H	Solid	Metallic Bonded Solid/modest shape change (5000 Atm)/SBB
10	850	Ar	Solid	Only powder remains/WBB
11	850	Ar	Solid	Retest of 10, only powder remained (confirmation run), WBB
12	750	Ar/H	Solid	Metallic Bonded Solid/modest shape change (1000 Atm)/SBB
13	750	Ar/H	Solid	Metallic Bonded Solid/modest shape change (3000 Atm)/SBB
14	900	Ar/H	Solid	Metallic Bonded Solid/modest shape change (5000 Atm)/SBB
15	950	Ar	Solid	Poor Bonding lead to cracking (1800 Atm), WBB

2. Sample Mold

The molds are created from Grafoil (GTA Grade 0.3 mm thick, NeoGraf Solutions, Lakewood, OH, USA), a moderate surface area, $\sim 22 \text{ m}^2/\text{g}$, graphite material [26,27] made from compressed graphite flakes. This material has approximately the same mechanical properties as paper of the same thickness and can be cut and shaped like paper. Small imperfect cylinder molds approximately 1.0 cm in diameter (inner diameter) by 0.5 cm tall were easily created for each experiment to serve as a mold. In addition, to add mechanical stability, the cylindrical molds were placed in a “stand” also made of Grafoil. The stand consisted of 10 layers of Grafoil formed into a rectangle, approximately 4.5 cm x 1 cm. A hole was punched in the center of the stand to accommodate the cylindrical mold (Figure 2 and Figure 3).

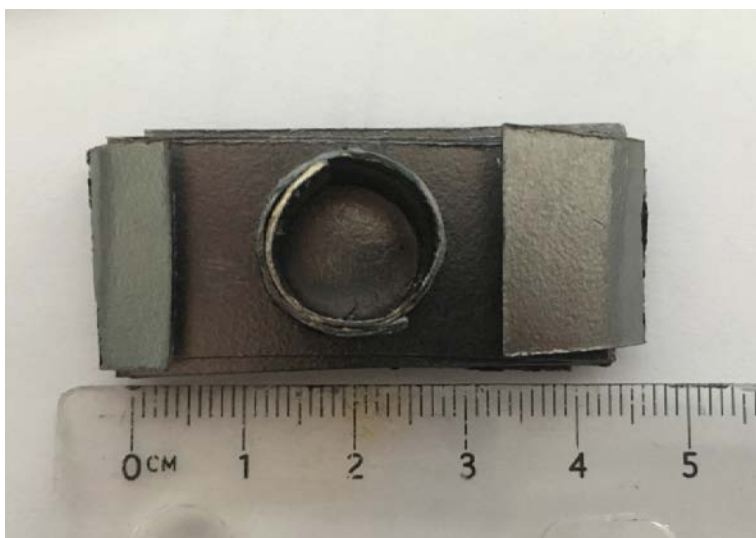


Figure 2. Sample mold: Top view

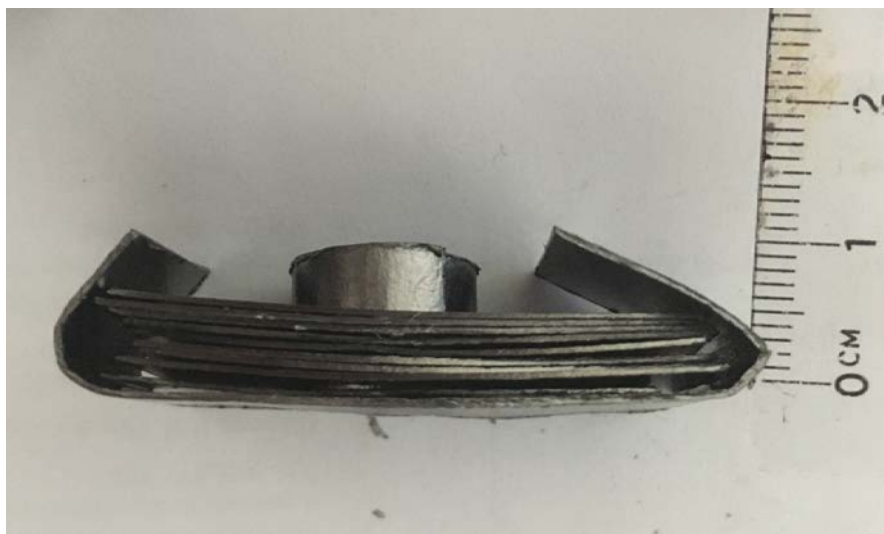


Figure 3. Sample mold: Side view

3. Sample in Furnace—Firing

Firing took place in a Lindburgh-Blue M 24” single zone furnace. The furnace was operated anywhere from 550 °C to 950 °C for this study. It can be seen in Figure 4.



Figure 4. Lindburgh-Blue M 24” Single Zone Furnace use for all samples

Firing was an eight-step process:

1. The mold and stand were placed in the center of a 50 cm × 2.5 cm diameter quartz tube.
2. Flushing was done using ultra-high purity (UHP) argon (Praxair, Salinas, CA, USA) or a pre-mix gas of argon and 2% hydrogen (Praxair, Salinas, CA, USA). Gas was passed through the quartz tube at approximately 50 sccm for 30–50 minutes.
3. Gas flow was reduced to approximately 10 sccm.

4. The quartz tube was placed inside the tube furnace (Lindburgh-Blue M 24" single zone) pre-heated to the test temperature. The tube was placed such that the mold/sample was at the furnace center.
5. The quartz tube/sample was held at the test temperature with constant gas flow (usually 4 hours but up to 12 hours).
6. After the allotted test time, gas flow increased to 50 sccm and the tube was quickly removed from the furnace.
7. The quartz tube/sample cooled under gas flow and at ambient temperature for 50 minutes. This long cooling period was for safety as well as to prevent potential oxidation of the samples.
8. Once cooled, the sample was removed for observation.

Throughout all testing, this process was consistent. The only deviations from one test to the next was firing time, flow type (pure argon or an argon/hydrogen mixture), and temperature.

4. Materials Characterization

To analyze the success of each sample prepared via HEAT as well as the control samples prepared in pure argon, various materials characterization techniques were employed. The primary methods were TGA, XRD, SEM, Ohaus density tests, and Instron compressive tests. Additionally, qualitative hardness measurements were observed and recorded.

a. Thermal Gravimetric Analysis

Thermal gravimetric analysis is a technique “in which the mass of a substance is monitored as a function of temperature or time as the sample is subjected to a controlled temperature program in a controlled atmosphere” [28]. An example of a TGA can be seen in Figure 5.



Figure 5. Thermal Gravimetric Analyzer

The variables monitored by the system are initial and final temperature, heating rate ($^{\circ}\text{C}/\text{min}$), and atmosphere. The data that is collected is weight, time, and temperature [28]. The method by which the TGA generates controlled heating is through applying an alternating current across a “small piezoelectric disk of quartz” [28]. For this study, the TGA was utilized to determine the decomposition temperature of titanium hydride. That temperature was significant as it correlates not only to the temperature at which the titanium hydride decomposes, but more imperatively for HEAT, kinetically forms and decomposes.

b. X-ray Diffraction

X-ray Diffraction (XRD) is a characterization technique that takes advantage of elastic scattering diffraction patterns of x-rays to give information regarding sample composition and crystalline structure [29]. An XRD machine is capable of detecting sample composition, residual stress, and lattice structure [30]. Due to the nature of the research, sample composition was the most important parameter examined. The Rigaku Miniflex

600 X-ray diffractometer was used to determine sample composition. This device is featured in Figure 6 [22].



Figure 6. Rigaku Miniflex 600 X-ray Diffractometer

This XRD primarily produced X-rays with a wavelength of 1 angstrom [12]. This is significant as 1 angstrom corresponds to the interatomic spacing within crystals [12]. As a result, it gives the machine great capacity to interpret material characteristics. Bragg's Law describes the diffraction that occurs when an incident X-ray interacts with the sample. Bragg's law is displayed in Equation 1.

$$n\lambda = 2d \sin \theta \quad (1)$$

Equation 1 states that the product of the integer number, n , and the wavelength of the incident X-ray, λ , is equal to twice the distance between crystal planes, d , and the sine the diffraction angle, θ [12].

Due to constraints of the XRD itself, it requires that a sample be in powder form to analyze. As a result, the sintered samples underwent light abrasion to release surface particles to be collected and examined. The powder released from each sample was placed on an XRD carriage. A dimple in the center ensured the powder stayed in place. An image of the XRD carriage that held the sample can be seen in Figure 7.

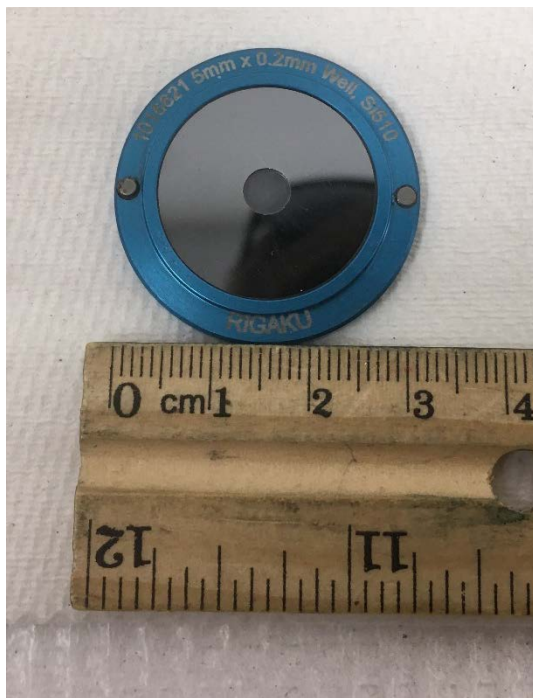


Figure 7. Mirrored sample carriage

For all samples analyzed, the parameters of the XRD were identical. These conditions can be seen in Table 2.

Table 2. XRD measurement conditions

X-Ray	40 kV, 15 mA	Scan Speed	5 deg/min
Filter	K-beta (x1)	Step Width	0.0100 deg
Detector	D/teX Ultra	Scan Axis	2 Theta/Theta
Scan Mode	Continuous	Scan Range	10-90 deg

c. Scanning Electron Microscopy

To image microstructures, the scanning electron microscope (SEM) was employed. Naval Postgraduate School operates the Ziess Neon 40 FESEM with attached energy dispersive spectroscopy (EDS) detector, presented in Figure 8. Key parameter settings were a 30 μm aperture and an accelerating voltage of 20 kV. The EDS was not used for any analysis as the XRD provided superior compositional characterization of the samples produced.



Figure 8. Zeiss Neon 40 FESEM and EDS. Source: [12].

The SEM is a “scientific instrument that use(s) a beam of highly energetic electrons to examine objects on a very fine scale” [31]. When compared to a traditional optical microscope, the scanning electron microscopes has unique range of capabilities that make it essential in material characterization. Topography, morphology, composition, and structure of a sample can all be determined via the SEM [31]. For all samples, Secondary Electrons (SE) provided the data required for imaging and analysis. SE are produced as a result of a collision between electrons within the primary electron beam and free electrons on or near the sample surface [12]. Following the collision, SE will be ejected from sample. The collection of the electrons by an internal sensor produces an image. Figure 9 displays SE production and other interactions that take place within the SEM.

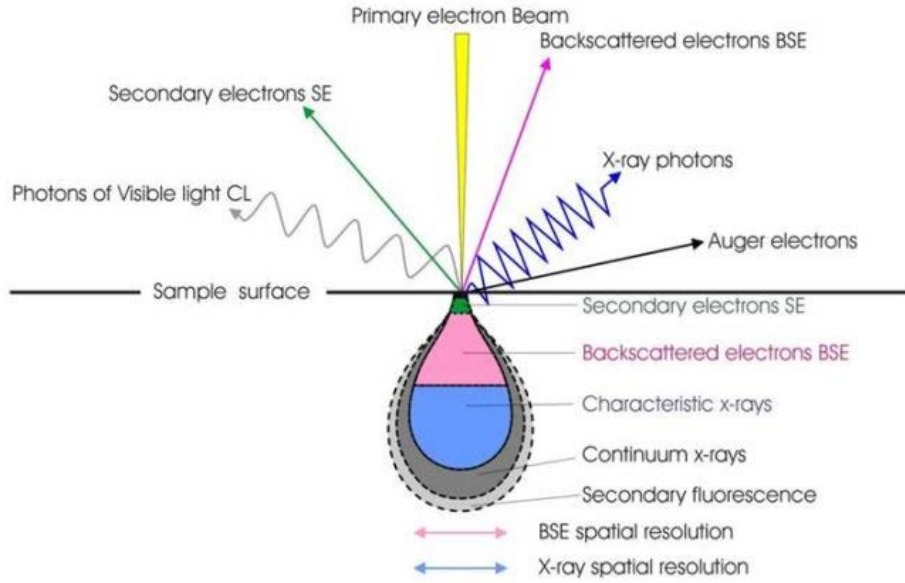


Figure 9. Specimen and electron interaction. Source: [31].

d. Ohaus Density Tests

To determine sample density, the Ohaus density kit was utilized. The Ohaus kit compares the scale readings before and after the sample is submerged in water to determine the samples approximate density. Equation 2 displays the analytical method used to determine sample density:

$$\rho_{sample} = \frac{A}{A-B}(\rho_0 - \rho_L) + \rho_L. \quad (2)$$

In this equation, “A” represents the sample mass prior to being submerged while ‘B’ represents the mass after submersion. The density of the submersion fluid, ρ_0 , and the density of air, ρ_L , are also factors in this equation. The difference in the measurement between A and B is as a result of the buoyancy force due to the object displacing the measurement fluid, water. The density determination kit can be seen in Figure 10.



Figure 10. Ohaus density test

Regarding the steps required to determine the density, additional equipment was needed. The first step was to determine the “dry weight” of the sample of interest. The scale displayed in Figure 10 was used to determine dry weight in grams. Following, the sample was submerged in water. A proprietary beaker provided by Ohaus must be used to ensure compatibility with the scale. This beaker can also be seen seated on the scale in Figure 10. Following, the beaker and submerged sample were put into a vacuum chamber. The chamber used can be seen in Figure 11.

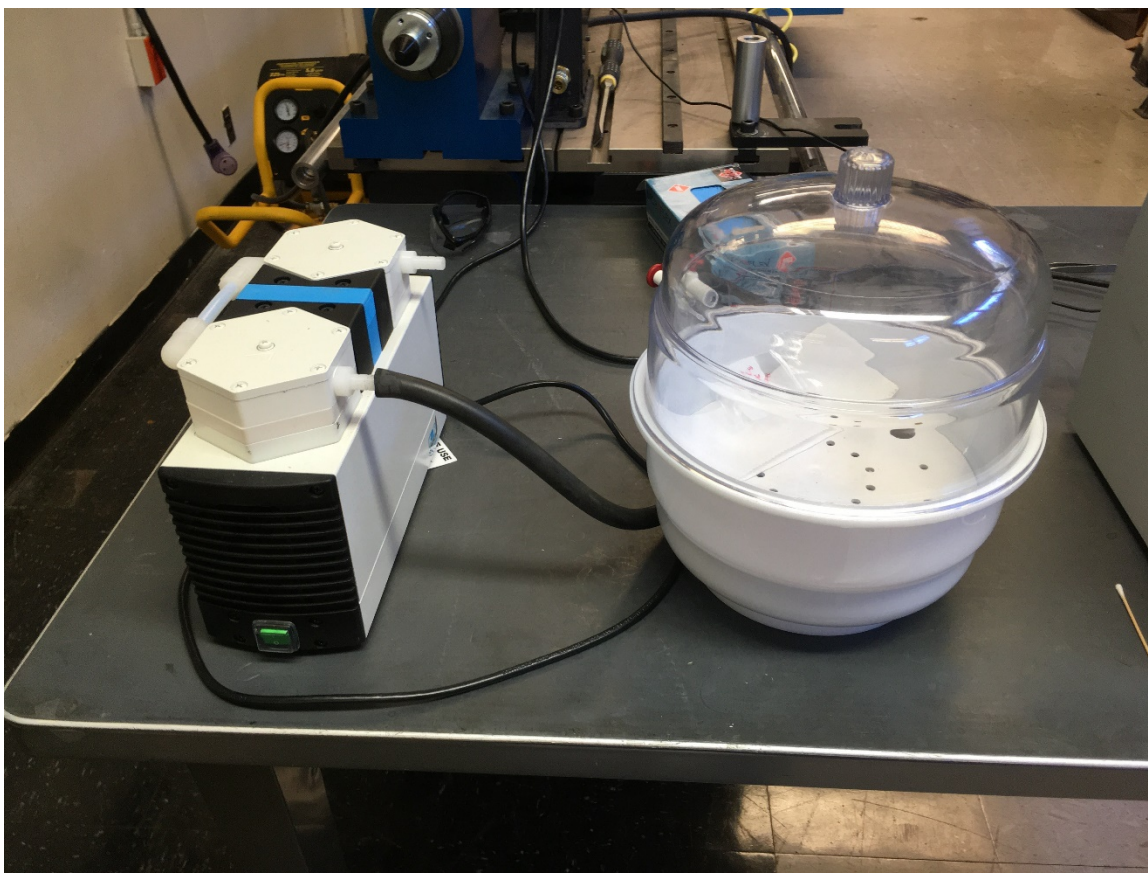


Figure 11. Vacuum chamber used for density analysis (L. pump, R. chamber)

The sample, still submerged in water, was then left in the vacuum chamber for 15 minutes to ensure that any air trapped on the surface was released from the sample. After releasing the vacuum, the beaker and sample were then inserted into a Fisher Scientific FS110 ultrasonic cleaning bath, Figure 12.



Figure 12. Fisher Scientific (FS110) Digital Ultrasonic Cleaning Bath

Rather than being use for cleaning, the ultrasonic bath was primarily used to release surface bubbles that had formed while the sample was in the vacuum chamber. Once again, the sample was moved to the scale. Ensuring that the sample remained submerged, it was lifted into the wire basket. This prevented any bubbles from forming due to atmospheric exposure. The final weight was measured. Ambient temperature and water temperature were both recorded in order to solve Equation 2.

e. Instron Compressive Tests

In addition to the non-destructive characterization techniques, intron compression, a destructive analysis technique, was also used. The primary purpose of compressive intron testing is to gain insight into a materials integrity under stress. Compressive testing, as opposed to tensile testing, was decided upon based on the use case of the titanium brown body. The brown body would not experience any tensile loads as it is not in its final fully sintered state, but compressive testing allowed for analysis that might resemble moving the brown body from one furnace to the next, or general transportation. Additionally,

compressive analysis is a common procedure when analyzing metal foam materials and although this research was not initially directed towards that end, it is good practice to have the results as they may give insight to future research.

The specific machine utilized for the compressive testing was the Instron 5982. The machine itself had a capacity of 100 kN, but 60 kN of compressive force was never exceeded in any test. The machine can be seen in Figure 13 and Figure 14.



Figure 13. Side-view of Instron



Figure 14. Front-view of Instron

The output of the compression test are time, force, and displacement. Although these values are useful, the qualities that hold more significance are the stress and strain values. To calculate stress and strain, the following two equations can be utilized:

$$\sigma = L/A \quad (3)$$

$$\varepsilon = \text{Disp}/\text{Length}. \quad (4)$$

Stress, σ , is equal to the load, L , over the surface area on which the load is applied. The strain, ϵ , is equal to the displacement over the length. These values can then be tabulated in a stress strain curve for further analysis. For materials that exhibit constant deformation, ultimate compressive strength is determined as a percent of their initial thickness (1%, 5% or 10%) [32]. Due to the small size of the samples produced in this research, the stress and strain data proved to be unreliable. Fortunately, analysis on the compressed samples could still be done via the SEM and density analysis equipment. Additional macroscopic observations were also recorded based on samples performance under a large compressive load.

C. RESULTS

The significant finding of this work was that the HEAT process, that is low temperature sintering of titanium particles in hydrogen gas, enables brown bodies of Ti/TiH₂ to form at ambient pressure and temperatures as low as 650 °C. The key results for sintering conducted in hydrogen forming gas (2% by vol H₂, 98% Ar) at ambient pressure are as follows:

- The titanium particles did not form solid bodies at temperatures below 650 °C.
- Brown bodies mimicked the shape of the graphene molds and would retain that shape given they were heated to 650 °C or higher.
- The brown bodies were primarily titanium metal but contained some TiH₂ as well.
- Although solid density was low (ca. 40%) all brown bodies could tolerate at least 5000 atm of pressure with no visible cracking and little strain. Brown bodies able to tolerate high pressure are labelled as strong brown bodies (SBB).
- High density metal was found to form during cold compression at lower pressure than normally required for titanium.

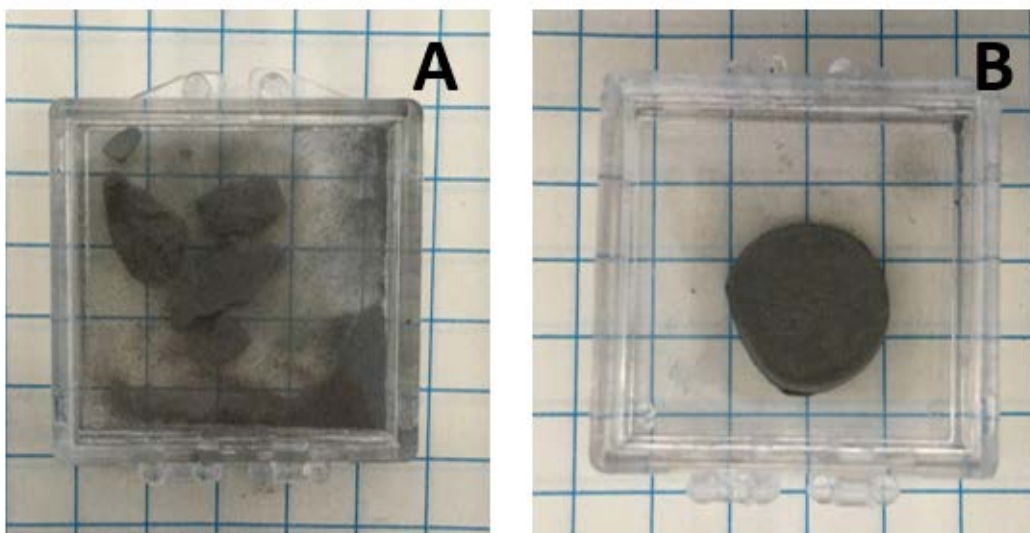
- Density increased with increases in firing temperature.

Samples sintered in argon only (control samples) were significantly different than those produced in forming gas. In particular, the following observations were noted:

- “Brown bodies” only appeared to form after heat treatments of 850 °C or higher.
- The apparent brown bodies were unstable. For example, samples produced at 850 °C completely decomposed to powder even after compression at relatively low (ca. 2000 atm) pressure. Samples produced at 950 °C in Ar did not pulverize at pressure, but large, easily visible cracks appeared even at 1000 atm. For this reason, these are labeled weak brown bodies (WBB).
- The WBB were 100% single phase of metallic titanium. Thus, control studies indicated that hydrogen gas was key to the observed low temperature sintering/strong brown body (SBB) formation observed in HEAT.

1. Visual/Macro Observations

Solid cylinders with the same radii as the mold formed above 650 °C for HEAT and above 850 °C for the control process. At lower temperatures, solid structures appeared to be present, but after modest shaking, only powder was left behind. The results of exposing samples to modest shaking highlights the structural integrity of the control samples to those prepared via HEAT, Figure 15.



A) Control sample, Ar only, 750 °C. Sample displays brittle behavior, breaks and “powderizes.”
 B) Sample, imperfect cylinder shape that mimics mold shape, created in Ar/H₂, same conditions, shows metallic behavior, remained intact after shaking. (Scale—4 lines/inch)

Figure 15. Stability after mild shaking

As seen, samples formed below 850 °C in pure argon flow, Figure 15A, would not have adequate stability to be used as a brown body and undergo any sort of physical transportation. The sample prepared via HEAT, Figure 15B, maintained its shape during modest shaking and did not lose any bulk material.

2. TGA

The thermal gravimetric analyzer provided essential information regarding the decomposition temperature of titanium hydride. The parameters can be seen in Table 3.

Table 3. Parameters for XRD run

Sample	Temp Range	Atmosphere	Rate
Pure Titanium Hydride	0 °C – 1100 °C	Argon	30 °C/min

The output of a TGA run can be seen in Figure 16. The most significant result of the 3 lines presented is the solid green, mass change.

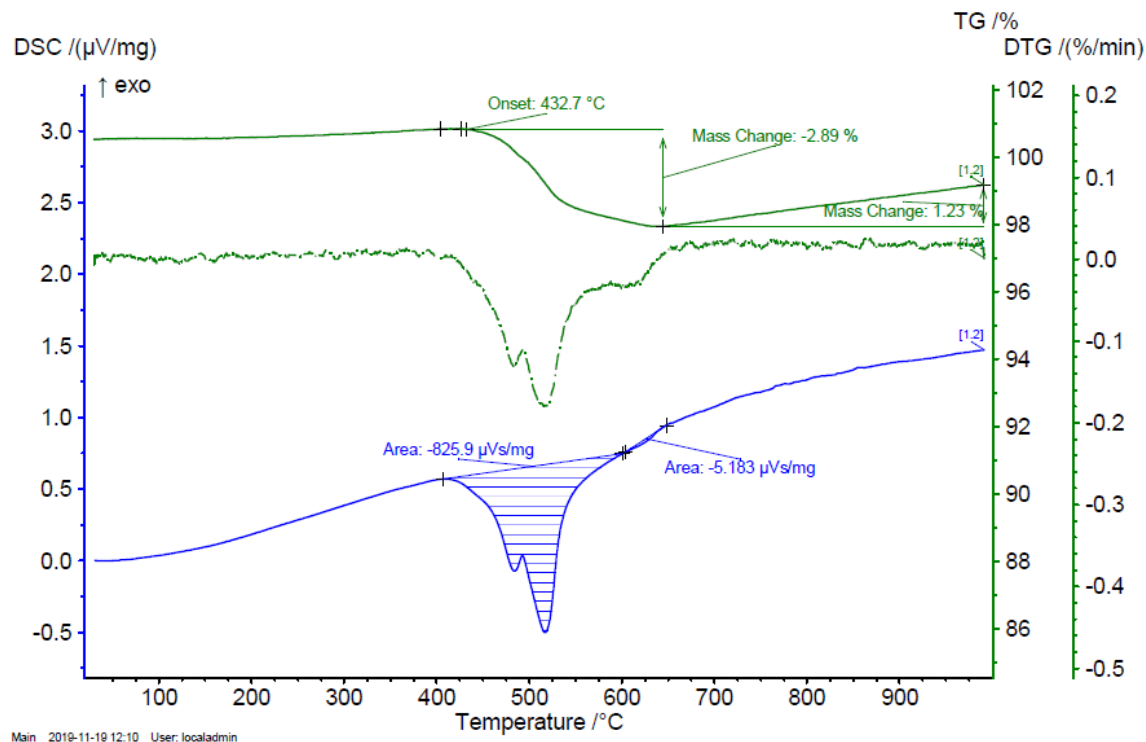


Figure 16. TGA results

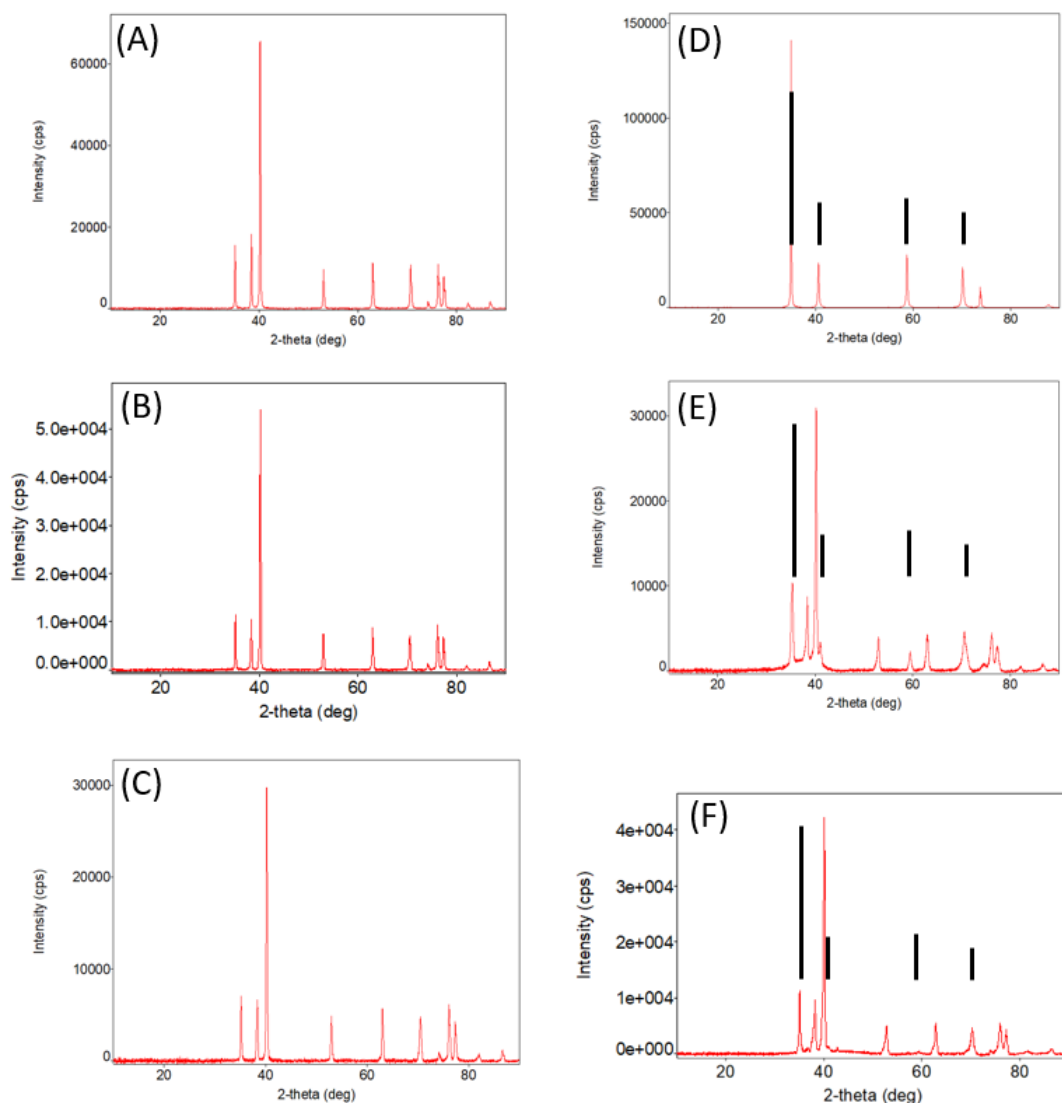
The change in mass is the most significant curve for this analysis (solid green line). It shows that the onset of titanium hydride decomposition is at 432.7°C and continues through 650°C and beyond. One result that was initially perplexing, though, was the mass gain following the initial mass loss associated with dehydrogenization. This phenomenon was explained through a study on the nonisothermal dehydrogenation of titanium (II) hydride powders [33]. In this study, there was a decrease in mass to 96.5% of the of the gross mass at 700°C [33]. After this temperature, the mass of the system began to increase [33]. This was attributed to oxidation that was as a result of an imperfect vacuum, allowing oxygen to absorb into the titanium at high temperatures [33]. Due to the lack of XRD analysis of our sample following the TGA run, it can only be concluded that the mass gain may be attributed to oxidation of the sample. This would be as a result of a poor vacuum

allowing oxygen into the chamber, in the same fashion as the research presented [33]. Despite the uncertainty associated with the mass gain, Figure 16 along with confirmation from external research allows for certain conclusion that dehydrogenization is a kinetic process which occurs between 432.7 °C and upwards of 650 °C [33].

As a result of this analysis, 650 °C was settled on as the starting temperature for analysis. Although other temperatures for firing were tested, 650 °C was significant as it was the lowest temperature at which significant quantities of titanium hydride would form and decompose. Additionally, it was also the temperature furthest from the traditional sintering temperature of titanium. This low temperature highlights the significance of the HEAT process.

3. XRD

The phases and percent mass of titanium found after treatment are clearly a function of the gas present during firing. After treatment in argon, at all temperatures, only titanium metal is present (Figure 17B and C). In contrast, after heat treatment in forming gas, although the spectra are dominated by metal peaks, there is always evidence of TiH₂ phases (Figure 17E and F). In fact, the difference between line positions for titanium and titanium hydride is slight, hence, the expectation is that the primary difference between a spectrum of pure titanium and one containing a few percent of TiH₂ will be i) line shape distortion/broadening ii) modest changes in relative peak intensity and iii) baseline shift. All of these features are found in the spectra of material treated in forming gas. For a comparison of pure titanium and titanium hydride, reference Figure 17A and D.



(A) represents the pure titanium sample while (D) represents the pure titanium hydride sample. Sample (B) is test 7, formed in pure argon at 750 °C. Sample (C) is test 11 which was formed in pure argon at 850 °C. Sample (E) was test 4, formed in Ar/H flow at 650 °C. Sample (F) is test 17 which was formed in Ar/H flow at 850 °C.

(B–C) Samples fired in argon and are pure titanium

(E–F) Samples fired in forming gas clearly contain both titanium and titanium hydride

Figure 17. XRD analysis of raw material (A, D) and solid samples (B, E, C, F)

The results presented in Figure 17 are significant as they prove that the flow of hydrogen leads to the production of titanium hydride in the sample. Samples B and C were formed at 750 °C and 850 °C respectively, in pure argon. Following the furnace run, both samples displayed an identical spectrum to that recorded by pure titanium, sample A. On the other hand, both sample E and F were produced in forming gas at 650 °C and 850 °C respectively and have a spectrum that is a mix of that produced by pure titanium, A, and pure titanium hydride, D. This proves that titanium hydride is dynamically created in the samples exposed to hydrogen flow at elevated temperatures.

The black bars present on the right-hand side of Figure 17 are representative of the relative intensities of pure titanium hydride (Figure 17D). As the bars are propagated through the samples formed with hydrogen present (E and F), slight influences of the titanium hydride can be seen in their representative spectral lines. This is indicative of a low percentage of titanium hydride in a predominantly titanium sample.

Employing PDXL (Rigaku proprietary software) to determine phase fractions from integrated line areas yields an estimate after treatment in forming gas at 650 °C (test 4) of 5% titanium hydride and 95% titanium. After treatment in forming gas at 850 °C, this method yields an approximate composition of 30% titanium hydride and 70% titanium. Although the absolute values are only roughly quantitative, the method does provide a valid qualitative indication that the amount of hydride increases with firing temperature.

4. Ohaus Density Analysis

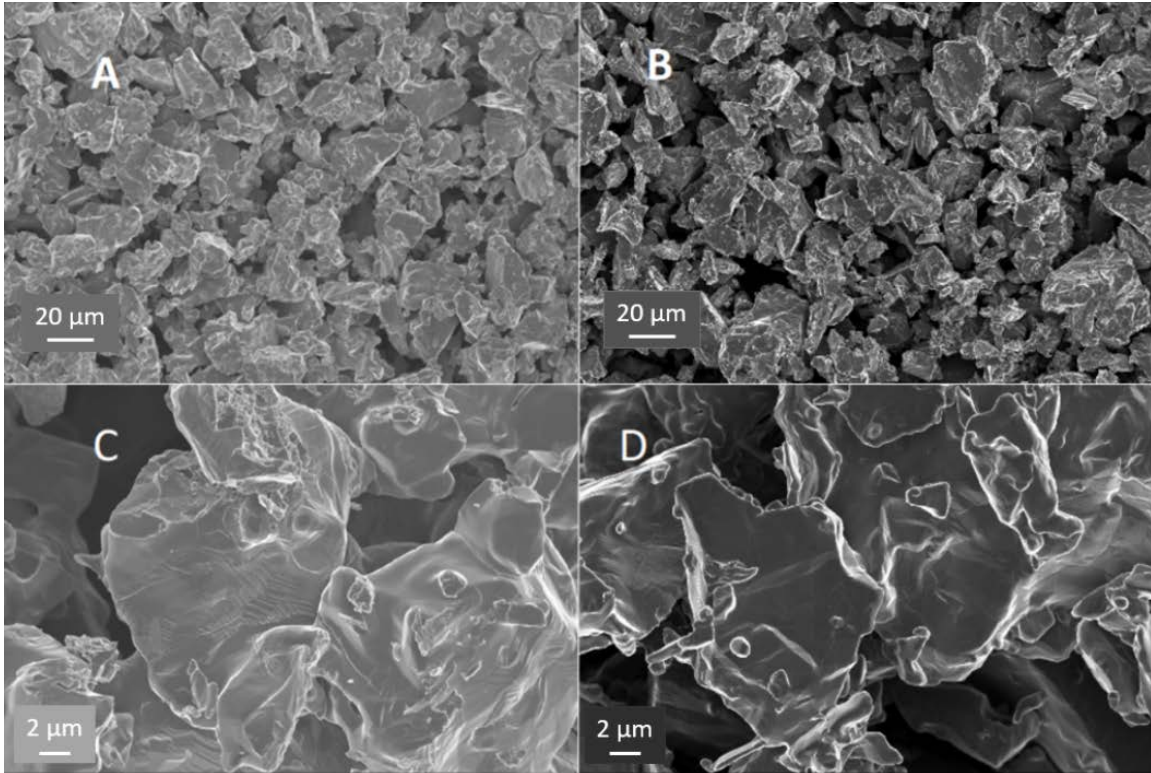
As shown in Table 4, the gross density of the strong brown bodies formed is very low at all temperatures, but there is a trend toward increased density with increased firing temperature. These samples, despite low fraction solid, are stable, and resist mass loss under normal handling.

Table 4. Density of samples fired in forming gas—Not compressed

Test	Firing Temp (°C)	Density (g/cm ³)	Fraction Solid
1	650	1.44	0.32
6	750	1.786	0.396
8	850	1.919	0.426
12	750	1.659	0.368
13	750	1.652	0.367
14	900	1.668	0.370

5. Scanning Electron Microscope

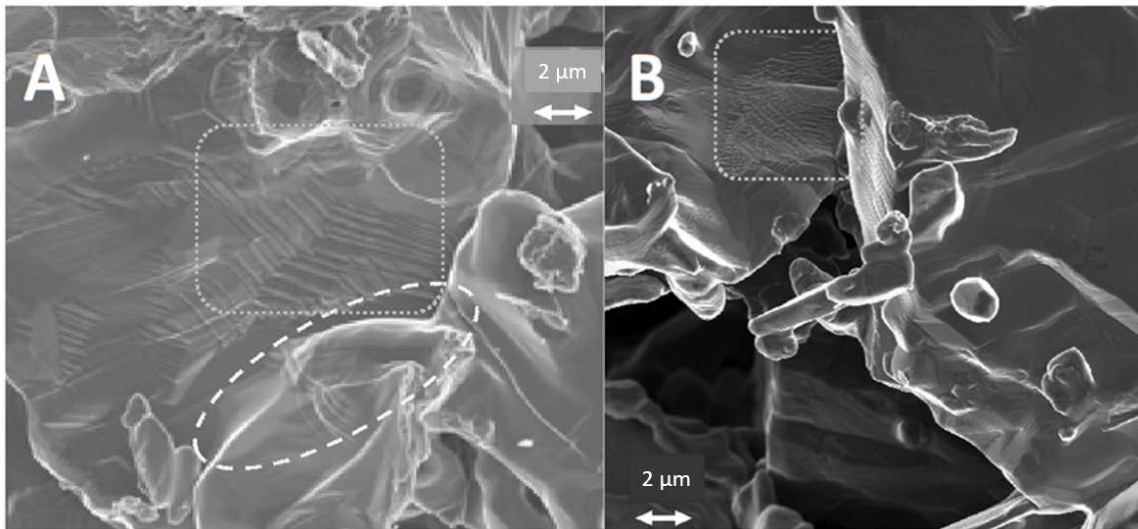
The SEM images support the proposed model of HEAT; however, the evidence is subtle. Unlike the very evident inter-particle necking observed in earlier RES-SM studies [2,11] of solid, designed shapes, formed from metal/metal oxide particle mixes using the RES-SM method, there are only subtle differences observed between samples prepared in Ar/H₂ mixes (HEAT process) relative to those created in Argon only (control) under otherwise identical conditions (Figure 18). Chief among the differences is the “softer” profile of the particles formed in Ar/H₂ mixtures, the identification of direction joining of some particles, and the appearance, only for the Ar/H₂ treated samples, of structures associated with multiple phases.



A and C.) HEAT at 850 °C. B and D.) Argon only 850 °C. HEAT samples show metal flow, ‘softer’ particle edges, evidence of sintering between particles, and examples of stacked layers (center of C), characteristic of titanium alloys with multiple phases.

Figure 18. SEM images of samples prepared with and without hydrogen

All of the above listed differences between Ar/H₂ and Ar only treated samples can be observed in Figure 18 and are even more evident in Figure 19. First, the micrographs suggest “rounding” of all particle edges in the HEAT processed cases. This structure is consistent with prior studies of particles growing via OR type sintering [13–16]. In those works, the same “rounding” of edges is observed. Also, only for the HEAT prepared samples is there evidence of chemical connections between particles. The structures observed are not “necks,” but clearly show “flow” between adjacent particles at particle edges. Finally, only the HEAT samples are there classic “stacking” structures observed in multi-phase titanium alloys [34].



Sample A was prepared with Ar/H₂ and shows evidence of sintering (ellipse area) and “stacked layers” (rectangular area). Sample B was a control sample prepared in pure Ar and shows small wrinkles/crenulations (rectangular area), but no evidence of sintering, stacking, or growth in SEM images.

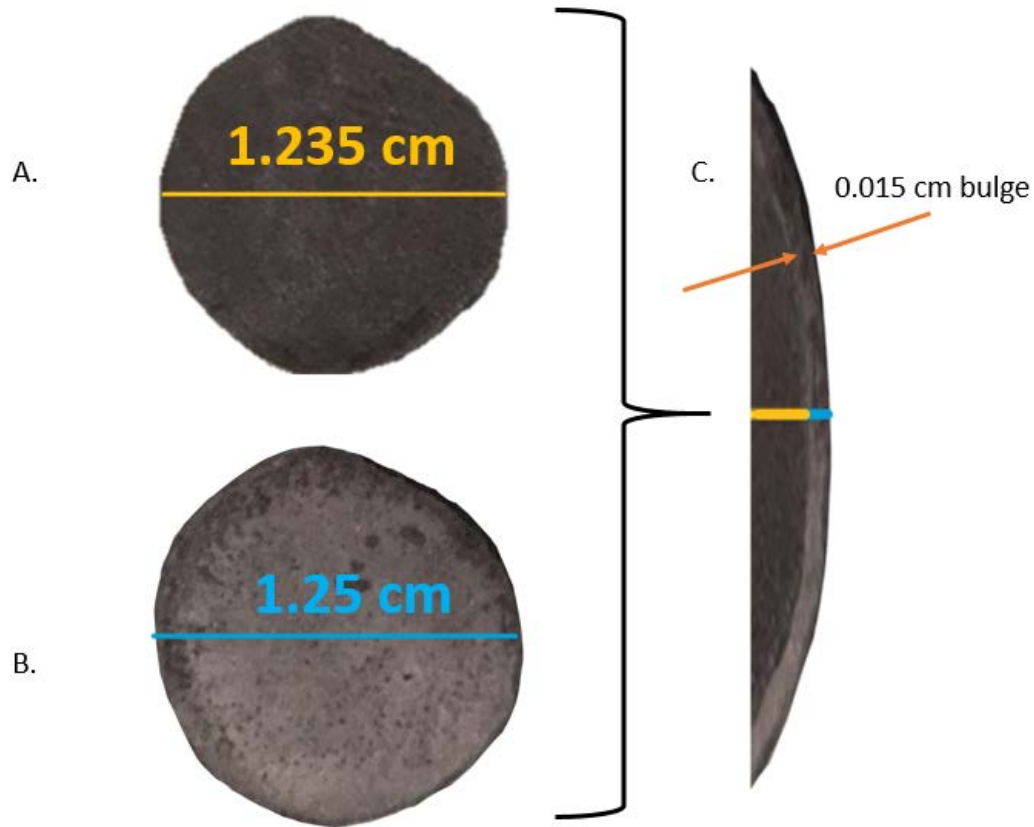
Figure 19. Features dependent on hydrogen flow

None of the features of the SEM results are inconsistent with the other findings. First, it is clear that there is a great deal of void space, in agreement with density studies (Table 4). Second, the XRD results (Figure 17) clearly indicate that there are multiple phases present in the HEAT samples. Third, following shaking (Figure 15) and compression studies (Figure 20 and Figure 21) only HEAT samples are evidently held together by metallic bonds throughout. The HEAT samples are stable to shaking and only metallic bonds can explain the plastic deformation observed under high pressure. In contrast, the thermally sintered control samples shatter in a brittle fashion under shaking or compression (Figure 15 and Figure 21).

6. Instron Compression

In the absence of a mold, compressed HEAT generated SBB demonstrate the existence of metallic bonding. As illustrated in Figure 20, the brown bodies sintered at 750 °C were modified in shape by high pressure compression (approximately 5000 atm), but only modestly. The diameter of the near cylinders, increase by roughly 2.5%. These modest dimensional changes are indicative of metallic bonding holding particles together throughout the sample. In contrast, WBB samples made by sintering in pure argon at

750 °C were found to be brittle. Even after relatively low loading (ca. 1000 atm) the samples completely crumbled (Figure 21). This indicates true metallic bonding did not exist in the control samples.

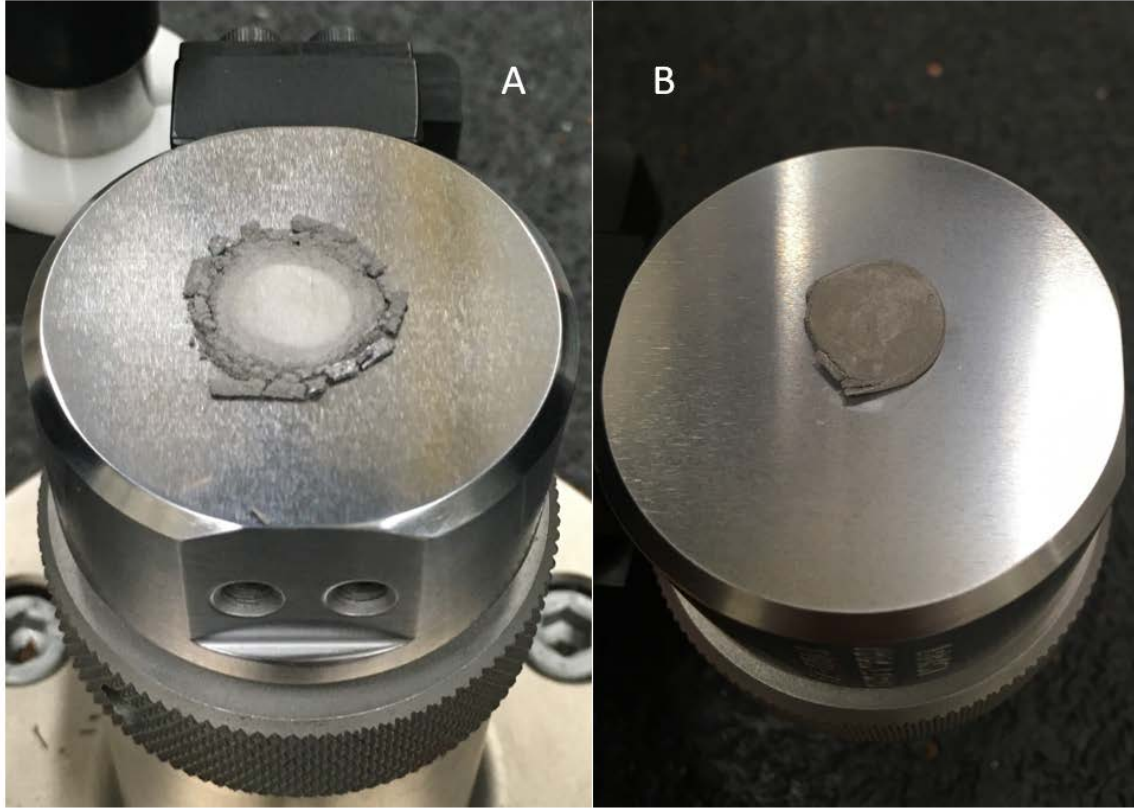


A) HEAT prepared sample prior to compression B) Same sample following approximately 5000 atm compression C.) Overlay of pre and post compression—diameter of specimen increased by approximately 2.5%.

Figure 20. Compression distortion

It is interesting to compare the density versus the compressive force data for the HEAT samples with earlier reports reporting the use of cold compression to create brown bodies from titanium and titanium hydride powders [35,36]. It must be noted in making the comparison, many earlier reports use titanium hydride, not pure titanium, and that all prior studies utilized solid molds during compression. Hence, it is anticipated that the earlier outcomes (Figure 22) can only serve as a point of qualitative comparison. In some cases,

the difference in protocol between the present work and earlier work can lead to enormous variation in observed behavior. For example, the absence of a mold for the control samples in the present study is likely cause for the observed brittle behavior.



A) Control sample formed at 750 °C, compressed to 1000 atm. It is clearly brittle and is pulverized during compression. B.) HEAT formed at 750 °C and compressed to 5000 atm. Retained its shape throughout compression.

Figure 21. Comparing crushed samples

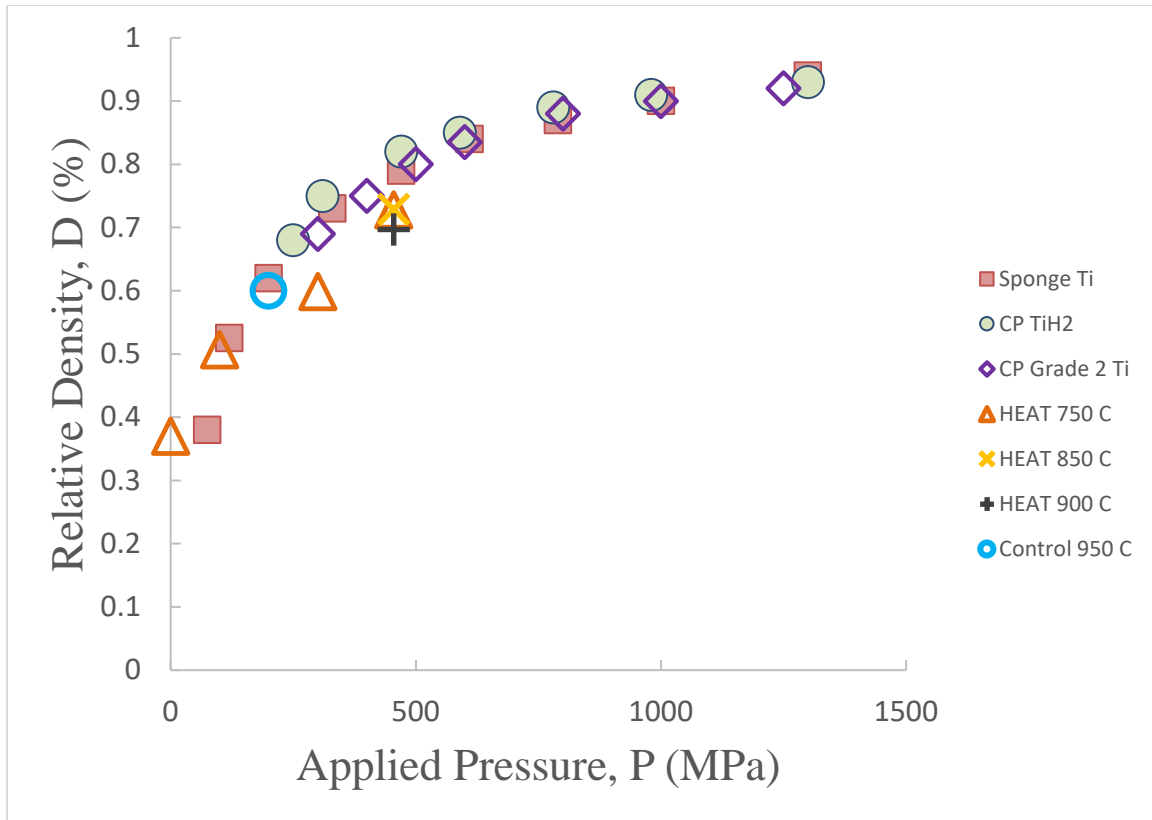


Figure 22. Density as a function of applied pressure at ambient temperature. Adapted from [35].

From this figure, it can be concluded that the SBB followed expected trends with regards to density associated with compression. It is important to remember, though, that the trademark for this study is the production of a SBB in the absence of compression or any atmospheric manipulation, such as a vacuum. Additionally, the only control sample that was able to withstand compression was that which was formed at 950 °C. Figure 22 is a testament to the durability of samples formed via the HEAT process.

Compression of control samples offered further evidence of the added stability produced by use of forming gas as a statement to the fragility in the absence of hydrogen. Indeed, WBB formed at 850 °C could not be “successfully compressed” using the mold-free protocol. WBB samples broke and “powderized” during the process (Figure 21A). Hence, it was not possible to plot the WBB data.

III. THE CONTRIBUTIONS OF TITANIUM HYDRIDE

Chapter II explores the research conducted utilizing titanium hydride and titanium/titanium hydride mixtures as precursors for the HEAT process.

A. INTRODUCTION

Titanium powder is the primary focus of research for thesis Chapter II, however titanium hydride/titanium mixtures were the original target for the study. The original experimental design for this thesis was based on this hypothesis: Given earlier reports that titanium hydride reduces the sintering temperature [22–25], the newly developed HEAT process in combination with titanium hydride will allow sintering at a lower temperature than pure titanium powder or even mixtures of titanium and titanium hydride. Due to the fact that testing with titanium hydride only took place at 650 °C, only a partial conclusion can be made; As described below, experimental work indicated that titanium hydride's partial addition in the precursor mix had no measurable impact on HEAT processed samples at 650 °C. Thus, it is tentatively concluded that at the low temperatures employed for HEAT (ca. <850 °C) earlier reports that TiH_2 is a “sintering aid” are not valid.

Contrary to the predictions of the original hypothesis, all data is consistent with this understanding: samples that utilize titanium hydride do not have a measurable difference when examining the macroscopic qualities and relative stability compared to a pure titanium counterpart. This is consistent with the postulated mechanism of the enhanced sintering observed in the HEAT process. To wit: the kinetic formation and degradation of titanium hydride is keystone ensuring transport of titanium atoms or clusters takes place in the bed. Hence, the similarity of results for titanium powder only and titanium mixed with titanium powder indicate that during the HEAT process, short lived, mobile titanium species, TiH_x , will form and decompose.

Still, there are significant advantages to using titanium hydride over pure titanium. The first advantage is the formability of titanium hydride. We found that titanium hydride can be formed into a shape, and will hold that shape, with minimal pressure. Titanium powder, on the other hand, is more dependent on a mold to maintain its shape. Second,

titanium hydride powder is less expensive than pure titanium powder [23]. The variation in price between pure titanium and titanium hydride is a byproduct of the titanium manufacturing process itself; the “low cost in titanium powder metallurgy (is) because titanium hydride such as TiH_2 is an intermediate product in the hydrogenation—dehydrogenate (HDH) process of titanium sponge” [37].

B. BACKGROUND

As mentioned previously, the combined influence of prior RES studies done at Naval Postgraduate School (NPS) as well as studies pertaining to the use of titanium hydride as a sintering aid led to the formation of what eventually became the HEAT process. There were four sources that were foundational to the generation of HEAT as a modification of RES-SM. Each will be explored individually regarding the topics those studies discussed as well as the impact of their research on this study.

The first study of interest regarded the use of titanium hydride as a sintering aid for the creation of alloy automotive components [24]. “The use of titanium hydride powder as a raw material has provided the right conditions for obtaining an alloy for automotive components, and allowed that the densification process has been performed at lower sintering temperatures than those required in the case of alloys based on pure titanium” [24]. This statement is significant as is, but in the context of success with prior RES studies [11], the intent of the work conducted for this thesis was to demonstrate that titanium hydride aids in the formation of solid titanium bodies from powders at lower temperatures and pressures than previously found possible.

In the automotive parts study, small amounts of Mn, Al, Sn, Zr, and C were incorporated as alloying elements in their titanium bodies [24]. In addition to having a wider array of used materials, the study also had much different testing parameters than explored in our research. With regard to pressure, the samples underwent 600 megapascals of compression prior to heating in pure argon [24]. With regards to heating, the samples were baked at temperatures above 1000 °C and up to 1150 °C [24]. It is notable, despite the application of high pressure, that in no case was the final product 100% dense. Despite the obvious differences from the study conducted and this thesis, a comparison clearly

indicates the advantages of the HEAT process: no high pressure required vs. 600 MPa, a lower required temperature for HEAT ($> 650\text{ }^{\circ}\text{C}$) vs. $>1000\text{ }^{\circ}\text{C}$ for earlier protocols [24].

In the second study [25], the use of titanium hydride as a sintering aid was further explored. In that study, only titanium and titanium hydride powders were employed, and they were never mixed. Like the first study, pressure was applied, nearly 9 megapascals, to create a body prior to firing [25]. Rather than using an inert gas flow, the samples were baked under high vacuum. The temperatures ranged from $1150\text{ }^{\circ}\text{C}$ to $1250\text{ }^{\circ}\text{C}$ [25]. The conclusion was similar to the first study: Titanium hydride powder sinters better than pure titanium powder. A final density of up to 98% was achieved when employing titanium hydride powder, but only 89% was achieved with pure titanium powder [25].

The third study was significant as it gave insight into how a variable composition blend of titanium and titanium hydride contributed to the relative density of the final product [23]. In all cases, a compression of 400 megapascals was applied to the powder prior to being put in the furnace [23]. All samples were exposed to $1000\text{ }^{\circ}\text{C}$ for 2 hours under pure argon flow. The highest relative density was again achieved when using exclusively titanium hydride rather than any mix of titanium hydride and pure titanium [23]. The conclusion of this test was similar to the articles already presented: As a result of using titanium hydride, it was possible to have a higher density at lower sintering temperature with better mechanical properties in comparison to that provided by a pure titanium sample [23]. The most significant conclusion of this study, though, might be that regardless of the percent of titanium hydride in the initial sample, after baking the percent hydrogen in the bulk material was consistent [23]. To be specific, their tests concluded that the final product was between “0.1 and 0.2 wt. %” hydrogen regardless of the initial ratio between titanium and titanium hydride [23]. This conclusion gives insight to the future findings of our study in that titanium hydride did not appear to have a significant effect on the sample’s mechanical properties as long as it was exposed to a hydrogen flow during baking.

The final study explored the contribution of pre-firing compaction on the relative density of the final sample. The compaction varied from 100 to 700 megapascals for both pure titanium and pure titanium hydride samples [22]. The temperature for all tests was

1350 °C and the dwell time in the furnace was four hours under a vacuum [22]. The results of the study showed a higher relative green density for pure titanium, but after firing, the titanium hydride had a significant advantage despite a lower green density. The density range of all tested titanium hydride samples was between 98.4-99.0% (100 MPa-700MPa) while pure titanium came in at 95.6-97.3% (100 MPa-700 MPa) [22]. These results proved the relationship between pre-firing compression on eventual density but also the impact of titanium hydride on sintering. “The densification of the TiH₂ specimens is obviously higher than that of Ti samples” is a conclusion that, through these studies, has come to be expected [22].

C. EXPERIMENTAL METHODS

It is important to reiterate that the HEAT process did not differ in any way when examining the products produced by pure titanium, titanium hydride, or a homogenous mixture of both. For all variations, the first step is to place only metal particles in the mold. Secondly, the metal particles were exposed to gas flow within a quartz tube. The flow was composed primarily of an inert gas (argon) and in some cases, a low percent of hydrogen. Following a flushing period, the gas flow was lowered and the tube enclosing the molds was inserted into a furnace at or above 650 °C. After the allotted baking time (30 minutes–12 hours), the tube was removed, the flow was increased, and the sample was allowed to cool for 30 to 50 minutes depending on furnace temperature.

From herein, only aspects of testing and analysis that differed from the pure titanium testing will be discussed.

1. Precursors

In Chapter I, only pure titanium was utilized, whereas in all tests undertaken for this study, the precursor consisted of a combination of pure titanium powder and titanium hydride. Figure 23 displays the titanium hydride used for all tests.



Figure 23. Sigma Aldrich – Titanium (II) hydride, 325 mesh, 98% metal basis

The temperature, flow type, time, and percent composition of each test can be seen in Table 5. Additionally, under the observation (Obv.) column an abbreviated description of the sample is given. For this column, SBB, WBB, traditional brown body (BB), and powder (PD) are used to describe a sample. A traditional brown body is a sample that did not undergo either compression testing or rigorous structural stability analysis. With that said, all BB did not break apart following removal from the mold, like a WBB sample would have.

Table 5. Testing parameters for all test using titanium hydride

Test	Firing Temp (°C)	Flow	Firing Time	Ti %	TiH ₂ %	Obv.
16	650	Ar	20 min	79.5	20.5	PD
17	650	Ar/H	20 min	78	22	BB
18	650	Ar/H	40 min	78	22	BB
19	650	Ar/H	3 hr	78	22	SBB
20	650	Ar/H	12 hr	78	22	SBB
21	650	Ar/H	12 hr	80.6	20.4	SBB
22	650	Ar/H	12 hr	79.52	20.48	SBB
23	650	Ar/H	12 hr	79.77	20.23	SBB
24	650	Ar/H	4 hr	20.22	79.77	SBB
25	650	Ar/H	4 hr	20.22	79.77	SBB
26	550	Ar/H	4 hr	20	80	BB

Some tests were completed more than once to ensure reliability of the results achieved, such as in test 24 and 25.

2. Sample Mold

The sample mold utilized for the titanium hydride testing was identical to that expressed in earlier in the report for pure titanium. In general, the mold was cylindrical and had a diameter of just over 1 centimeter.

3. Furnace

The furnace utilized in testing, again, is the same as utilized for the pure titanium testing. Although temperature and bake times varied, the protocol was identical. Any variation related to the furnace temperature or time can be seen in Table 5.

4. Materials characterization

The techniques used for materials characterizations were identical to those presented for pure titanium. Material characterization of the titanium/titanium hydride brown bodies was performed using the X-ray diffraction machine (XRD), scanning electron microscope (SEM), XPR/XSR Ohaus density test, and Instron tensile/compressive machine. A more in-depth analysis of these machines can be reviewed in the previous chapter.

D. RESULTS

The conclusions derived from titanium hydride testing similar, but more limited than that described for pure titanium. Whether the precursor is titanium or titanium hydride, if either element is exposed to a temperature of 650 °C with a hydrogen and inert gas flow, a solid body will form. For a confident analysis of titanium hydride, though, further testing at higher temperatures as well as a focus on more control studies (in pure argon) should be conducted. With that, a great deal of information was gathered from the samples generated.

1. Visual/Macro Observations

The titanium hydride formed solid samples that looked indistinguishable from those formed with pure titanium or a mixture of titanium and titanium hydride. The samples were made in identical molds so the diameter, although not entirely circular, was approximately 1 cm. Above 650 °C, the samples would hold their shape despite modest shaking. This was not true for the samples formed under pure argon. An example of a titanium hydride sample formed via HEAT can be seen in Figure 24.



When viewing a sample formed of pure titanium, titanium hydride, or a mixture of the two, they are indistinguishable in the absence of magnification.

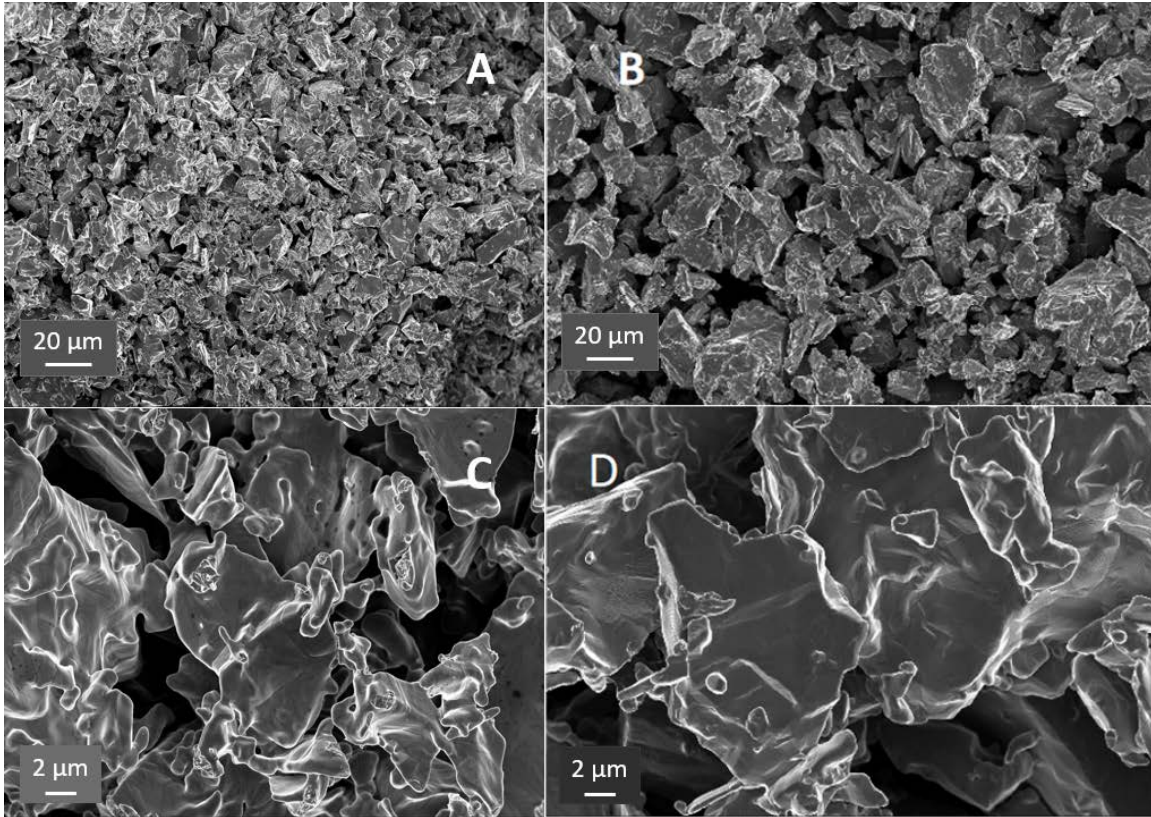
Figure 24. Titanium Hydride sample

2. TGA

The insight gained via the TGA, described in the first chapter of this report, was beneficial to both the pure titanium samples, pure titanium hydride samples, and mixtures. As determined by both TGA and eventual testing, 650 °C was the minimum temperature at which HEAT was a viable option for solidification.

3. SEM

Just as in the pure titanium studies, there is evidence for softer profile on the particles formed in argon-hydrogen gas flow as well as direct joining/sintering of some particles.



Sample A and C are the same sample—formed at 650 °C in forming gas with a 80% titanium hydride and 20% pure titanium by weight. Sample B and D are the control sample formed in pure argon at 850 °C.

Figure 25. SEM images prepared of titanium hydride in forming gas to a control sample prepared in argon

The same conclusions made for pure titanium can be seen in the titanium hydride sample, Figure 25A and C. Rounding of all titanium hydride particles took place during the HEAT process. Further imagine, revealed in Figure 26, shows a site where bonding between two adjacent particles took place.

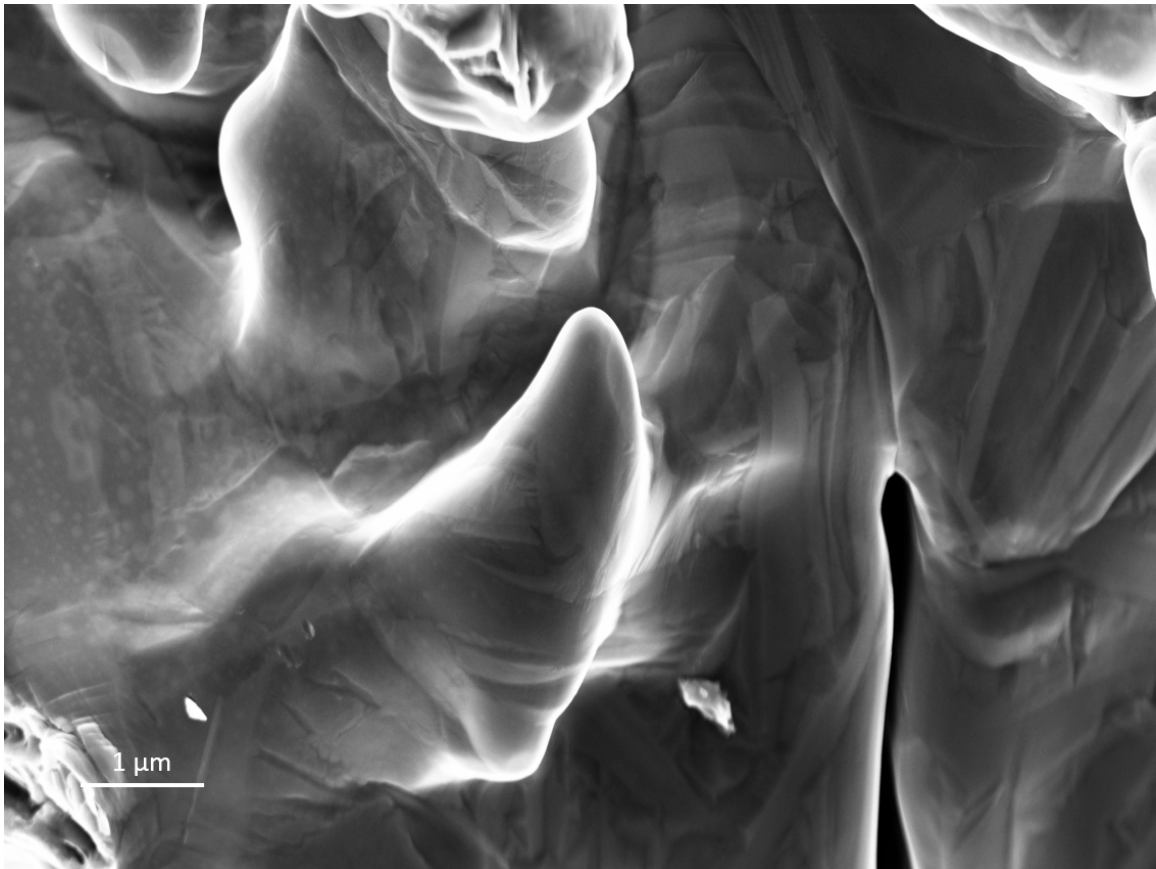


Figure 26. HEAT process leads to adjacent particles joining

These observations along with general handling qualities redefine the earlier statement: Solid titanium bodies produced through the HEAT process are held together by metallic bonds at significantly lower temperatures (200 °C or more) than that required for equivalent bonding in pure argon.

IV. DISCUSSION

All empirical evidence shows that the HEAT process leads to the formation of metallic bonded titanium brown bodies of any desired shape (matching the mold) from titanium particles treated at ambient pressure and temperature as low as 650 °C. The temperatures required to create these brown bodies are significantly lower than those employed in prior work; $ca > 1000$ °C. Additionally, in these studies, at the very least, 80 atm of pressure was required [19–25]. In contrast, brown bodies generated in the control studies, that is samples prepared identically to HEAT process but in the absence of hydrogen flow, are very brittle. These samples even showed brittle characteristics when heated to 950 °C (distinct cracking).

The data suggests a simple model of the mechanism of metallic bonded brown body formation: Hydrogen gas creates a short-lived volatile titanium compound that mobilizes titanium atoms or clusters. Through decomposition, the released metal atoms re-bond with existing particles and this eventually leads to particle sintering and the creation of metallic “connections” between existing titanium particles in the bed. The process of sintering described is anticipated by one of the oldest models of particle growth: Ostwald ripening [13–16].

All observations are consistent with this model. First, visual inspections and simple “shaking” tests reveal that only brown bodies produced in the presence of hydrogen between 650 °C and 850 °C are mechanically stable. By comparison, a sample formed in argon requires firing at 850 °C or higher to begin showing signs of stability (as mentioned, cracking was seen under compression on a control sample formed at 950 °C). Second, XRD studies reveal that some titanium hydride is present in all HEAT prepared samples. This is clear evidence that TiH_2 is produced and persists in the samples, a finding anticipated by and consistent with the model. Note, another fact consistent with the model: The Ti/TiH_2 phase diagram [38] indicates both metal and hydride phases should coexist at the temperatures employed. Third, SEM reveals the existence of features such as softened edges and evidence of direct particle-particle sintering, anticipated by OR process. The existence of step structures observed in SEM, similar to structures observed in stabilized

multi-phase titanium alloys [38], is consistent with the XRD results showing the coexistence of metal and hydride phases in the HEAT samples. Fourth, the finding that HEAT prepared samples modestly plastically deform under pressure is clearly an indication that these samples have metallic bonds formed between particles. In contrast, the control samples completely shatter under pressure, revealing a lack of metallic bonding between particles. This clearly supports the supposition that hydrogen is needed to create metallic bonding.

In addition to the data reported being consistent with the provided model, a number of reports in literature agree with the postulate that short lived volatile metal containing species can lead to gross modification of metals [15]. The earliest reports of atoms/radicals restructuring metals were published more than 90 years ago [39–42]. Of relevance are reports that hydrogen atoms can restructure metal. The earliest report of hydrogen atoms restructuring metal dates to 1933 [43]. It was reported that hydrogen atoms restructured arsenic, antimony, selenium, tellurium, germanium, and tin. The ability of hydrogen atoms to volatilize/restructure metals was repeated more recently [44]. In an even more recent report it was found that in the afterglow of a microwave generated hydrogen plasma tin foils were completely reorganized to create a low density network of micron scale “strings” [45]. Remarkably, detailed study showed the final structure was also tin and the restructuring took place without any weight loss. All evidence suggests the restructuring occurred via metal transport in the form of unstable tin hydride. There are also several reports of the restructuring of platinum due to the action of “radical” species, formed homogeneously during the combustion process of both ethylene [15,16,46,47] and hydrogen [48,49] oxidation. Reportedly, these radicals react with platinum foils, films, catalysts etc., to create very short-lived volatile species. Upon decomposition, new platinum structures form and produce average crystal and or grain sizes that are dramatically larger than in the untreated precursor, suggesting an OR process. The net result is gross scale reconstruction over time, at temperature hundreds of degrees below melting, often clearly observed without any magnification.

In all published reports of hydrogen induced metal reconstruction, the emphasis is on the action of hydrogen atoms, not molecules. Is it possible that hydrogen atoms are the

actual active species in HEAT? In brief, detailed study of H atom formation and consequent chemistry on other metals suggests it is quite possible H atoms are key to the HEAT process. Information regarding the interaction between titanium and H-atoms is insightful. At low temperatures and in the presence of hydrogen, titanium is known to form titanium hydride of all stoichiometries [50]. In addition, these hydrogen atoms will diffuse rapidly within the titanium crystal [50]. It is also clear there are a multitude of titanium hydride stoichiometries, of formula TiH_{2-x} where x can be greater than one, are known to exist. This clearly indicates that titanium can “split” hydrogen molecules. Moreover, it is well known that platinum, palladium, and other noble metals can split hydrogen at even ambient temperature. Hydrogen atoms created in this fashion are used in catalytic isomerization reactions [51–54]. It has even been demonstrated that hydrogen atoms created in this fashion can diffuse through the gas phase, impacting processes downstream [55]. In sum, although there is no direct study of atomic forming diffusing on titanium at elevated temperatures, the suggestion is consistent with observations regarding atomic hydrogen formation and diffusion on other metals.

THIS PAGE INTENTIONALLY LEFT BLANK

V. FUTURE TESTING

The first recommendation for future testing would be to further explore the effects of titanium hydride on the sintering behavior associated with the HEAT process. The stated conclusion that there is no significant difference in sintering behavior with and without titanium hydride present, is a tentative conclusion. Both control studies in argon as well as higher and lower temperature studies with mixtures of titanium and titanium hydride as well as entirely titanium hydride samples should be completed. This will allow for a definitive conclusion on the contributions of titanium hydride in the HEAT process.

Another unexplored aspect of this research was in the production of a fully densified titanium product. This would require HIP. Much of this study explored the characteristics of each sample in its brown body form, but a whole study could be devoted to understanding the processes leading to a fully sintered sample as well as studying the sample itself following densification. Naturally, this testing would lend itself to a much more rigorous comparison to established titanium manufacturing methods.

In future testing, the application of the HEAT process on other elements should be explored. These elements should be ones that are too stable for reduction by radicals at high temperatures, such as aluminum. Just as RES inspired HEAT as applied to titanium, the same could be done for other, similar, metals.

In addition to examining the applications of fully sintered samples following HIP, there is an equally substantial amount of research that can be done with the sample as it is produced via HEAT (generally a porous Ti/TiH₂ sample). Cellular metals, or metal foams, are an exciting branch of research that utilizes a porous metal sample for “efficient absorption of energy, for thermal management and perhaps acoustic control” [56]. Possibly a more exciting application of metal foams, specifically titanium metal foams, is in the medical field. Due to its bio-compatibility, low reactivity, light weight, and high strength, titanium is a popular material for medical applications. One interesting requirement for titanium metal foams, though, is that to mimic bone tissue, porosity is a requirement as it allows for a “stable blood supply and ingrowth of new tissue” [57].

Current methods of producing titanium foams have attempted powder metallurgy but they require the HIP process and space-holder particles to ensure the production of a porous structure [57]. Much like other studies that exclusively explored the manufacturing process associated with pure titanium powders, compression of the titanium powder sample prior to HIP was also attempted [57]. The result, though, was still a sample that did not fully replicate bone samples due to a lack of irregularity in the sample. Bone structures have “variable porosity, size, and shape” and the powder metallurgy processes historically do not meet that requirement [57]. The HEAT process, however, does produce a porous sample with a level of irregularity. In addition, the HEAT process does not require HIP in the absence of a need for a fully densified sample (which for medical applications, a fully dense sample is not desirable).

In future testing, the viability of HEAT produced titanium brown bodies in medical applications should be explored. This type of research would require a more in-depth porosity analysis, energy absorption analysis, and deformation capacity under stress. Based on the current standing, though, there is great potential for HEAT produced titanium foams in the medical field.

VI. CONCLUSION

The overall objective of this research, to find a low temperature sintering mechanism for titanium powder, was successful. The research conducted proved that the HEAT process could generate a SBB at or above 650 °C in Ar/H flow. In addition, the questions regarding the potential applications of both a fully dense and porous titanium body were examined and the results are significant. As a porous body, the medical industry could use HEAT generated samples as bone replacements, potentially, without any further treatment. As a fully dense sample, HIP treated HEAT samples could be used in traditional structural applications, such as load bearing members in aircraft.

All data indicates that the HEAT process; specifically treating a mold filled with titanium particles to above 650 °C in a flowing ambient pressure gas containing hydrogen creates a metallic bonded brown body on the order of 40% metal density. The brown body will also mimic the mold shape. Based on prior work with titanium brown bodies formed using Ti-MIM [20] it is anticipated that second step of hot isostatic pressing will lead to complete densification.

The HEAT process may have advantages relative to current commercial processes. For example, HEAT creates a titanium brown body in a single step in a soft mold. In contrast, Ti-MIM requires a sequence of steps to create a similar brown body: i) mixing metal and binder, ii) high pressure injection and high pressure molds, iii) moderate temperature green body formation and iv) very slow debinding at 900 °C. Laser sintering from particles requires extremely expensive equipment, is slow, and requires significant expertise. Arguably, it is also not true additive manufacturing as those particles not sintered are removed from the bed after each multi-micron scale “level” is complete.

Finally, all data collected is consistent with a simple model: In the presence of hydrogen at temperatures exceeding 650 °C, some form of titanium hydride is produced. The vapor pressure is enough to carry titanium short distances within the bed before depositing. Titanium atom/clusters generated by the decomposition are released and these

bond with existing particle surfaces. The net result, as anticipated by the Ostwald Ripening model, is sintering and metal bonding between particles.

This work was designed for comparison with existing metal additive manufacturing technologies, particularly mold-based MIM. In MIM engineering as in true metal additive manufacture by laser sintering, the final part is required to be a fully dense metal object. Alternatively, the “brown” titanium parts created here can be considered “designed” open cell titanium/titanium hydride metal foams of high compressive strength. Cellular metal foams, as discussed elsewhere [56–62], may have properties for some applications superior to fully dense metal parts. For example, the light weight, yet high strength (Figure 22) of such foams could be advantageous for applications in aerospace and as bio compatible implants [56–62]. Thus, it is possible that the brown bodies of specific shape produce with the HEAT process may represent an end state for some applications with no need for further densification.

LIST OF REFERENCES

- [1] Phillips, J., 2017, "Systems and Methods for Low Temperature Metal Printing," U.S. Patent Pending 62/541,364.
- [2] Phillips, J. and Daniels, Z., 2018, "Reduction Expansion Sythesis of Sintered Metal," U.S. Patent Pending 62/778,785.
- [3] Zea, H., Luhrs, C., Phillips, J., "Reductive/Expansion Synthesis of Zero Valent Submicron and Nanometal Particles," J. Mater. Res., **26**, pp. 672.
- [4] Luhrs, C., Kane, M., Leseman, Z. and Phillips, J., 2013, "Novel Process for Solid State Reduction of Metal Oxides and Hydroxides," Metall. Mater. Trans., **44**, pp. 115.
- [5] Luhrs, C., Leseman, Z., Phillips, J. and Zea H.R., 29 April 2014, "Generation of Metal and Alloy Micron, Submicron or Nano Particles in Simple Rapid Process," U.S. Patent 8,709,126.
- [6] Luhrs, C. and Phillips, J., 25 November 2014, "Reductive/Expansion Synthesis of Graphene," U.S. Patent 8,894,886.
- [7] Lim-Lee, T., Adams, R.A., Luhrs, C., Arora, A., Pol, V. g., Wu, C. H. and Phillips, J., 2018, "High-Stability Tin/Carbon Battery Electrodes Produced Using Reduction Expansion Synthesis," Carbon, **132**, pp. 411.
- [8] Elbaz, L., Phillips, J., Artyushkova, K., More, K. and Brosha, E. L., 2015, "Evidence of High Electrocatalytic Activity of Molybdenum Carbide Supported Platinum Nanorrafts," J. Electrochemical Soc., **162**, pp. 681–685.
- [9] Pelar, C., Greenway, K., Zea, H., Wu, C.H., Luhrs, C. and Phillips, J., 2018, "Novel Chemical Process for Producing Chrome Coated Metal," Materials, **11**, pp. 78.
- [10] Phillips, J., 2019, "Chemical Methods to Create Metal Films on Metal and Ceramic Substrates," U.S. Patent 10,273,582.
- [11] Rydalch, W., Daniels, Z. Ansell, T., Luhrs, C. and Phillips, J., 2019, "Reduction Expansion Synthesis of Sintered Metal," Materials, **12**, pp. 2890.
- [12] Rydalch, W., 2019, "Reduction Expansion Synthesis of Sintered Metal," M.S. thesis, Materials Department, Naval Postgraduate School.

- [13] Alexandrov, D.V., 2014 “On the Theory of Ostwald Ripening: Formation of the Universal Distribution,” J. Phys. A., **48**.
- [14] Lifshitz, I.M. and Slyozoy, V.V, 1961, “The Kinetics of Precipitation from Supersaturated Solid Solutions,” J. Phys. Chem., **19**, pp. 35–50.
- [15] Wei, T.C. and Phillips, J., 1996, “Thermal and catalytic etching: Mechanisms for metal catalyst reconstruction,” Adv. Catal, **41**, pp. 359–421.
- [16] Wu, N.L. and Phillips, J., 1988, “Sintering of Silica Supported Platinum Catalysts during Ethylene Oxidation,” J. Catal, **113**, pp. 129–143.
- [17] Lutjering, G. and Williams, J. C., 2007, *Titanium*, Springer – Verlag.
- [18] Inagki, I., Takechi, T., Shirai, Y. and Ariyasu, N., 2014, “Application and Features of Titanium for the Aerospace Industry,” 106, Nippon Steel and Sumimoto Metal Technical Report.
- [19] Boyer, R., 2010, “Characteristics and Applications of Titanium and its Alloys,” J. Mater., **62**, pp. 21–24.
- [20] German, R.M., 2013, “Progress in Titanium Metal Powder Injection Molding,” Materials, **6**.
- [21] Ewart, P.D, 2018, “The Use of Particulate Injection Molding for Fabrication of Sports and Leisure Equipment from Titanium Metals,” Proceedings, **2**, pp. 254.
- [22] Wang, C., Zhang, Y., Xiaio and Chen, Y., 2017, “Sintering Densification of Titanium Hydride Powders,” Mat. And Man. Proc., **32**, pp. 517.
- [23] Hedayati, A., 2012, “Fabrication and Properties of TiH₂ and Ti Blends for Powder Metallurgy Ti Products,” M. S. thesis, Materials Science Department, The University of New South Whales.
- [24] Ileana, C., Stefan, G., Ilie, D. and Claudiu, N., 2016, “Aspects about Sintering Behavior of a Titanium Hydride Powder Based Alloy Used for Automotive Components,” Applied Mech. And Mat., **823**, pp. 467.
- [25] Lee, D. W., Lee, H.S., Park, J. H, Shin, S.M. and Wang, J.P., 2015, “Sintering of Titanium Hydride Powder Compaction,” Proc. Of Manuf., **2**, pp. 550.
- [26] Phillips, J. and Dumesic, J.A., 1981, Appl. Surf. Science., **7**, 215–230.
- [27] Phillips, J., Clausen, B., Dumesic, J.A., 1980, “Iron pentacarbonyl decomposition over Grafoil. Production of small metallic iron particles,” J. Phys. Chem., **84**(14), 1814–1822.

- [28] Ansell, T. and Claudia, C., 2019, “Thermal Analysis Lecture Notes FY20.”
- [29] 2018, “XRD Basics,” last modified February 28, 2018, accessed August, 2019, <https://www.physics.upenn.edu/~heiney/datasqueeze/basics.html>.
- [30] Seeck, O., Murphy, B., 2014, *X-Ray Diffraction: Modern Experimental techniques*, Pan Stanford Publishing, Boca Raton, Florida.
- [31] Ansell, Tory, 2019, “Microscopy Lecture Notes FY20.”
- [32] 2019, “What is Compressive Testing,” Instron, accessed February 27, 2020, <https://www.instron.us/en/our-company/library/test-types/compression-test>.
- [33] Liu, H., He, P., Feng, J.C., and Cao, J., 2009, “Kinetic on Nonisothermal Dehydrogenation of TiH₂ Powders,” *International Journal of Hydrogen Energy*, 34, pp. 3018–3025.
- [34] Denquin and Naka, S., 1996, “Phase Transformation Mechanisms Involved in Two-Phase TiAl-Based Alloys – I. Lamellar Structure Formation,” *Pergamon*, **44**(1), pp. 343.
- [35] Machaka, R. and Chikwanda, H., 2015, “Analysis of the Cold Compaction Behavior of Titanium Powders: A Compressive Inter-Model Comparison of Compaction Equations,” *CrossMark*, **46A**, pp. 12.
- [36] Machaka, R. and Chikwanda, H., 2015, “Analysis of the Cold Compaction Behavior of Titanium Powders: A Comprehensive Inter-Model Comparison Study of Compaction Equations,” *Metall. Mater. Trans. A*, **46**, pp. 4286–4297.
- [37] Mei, L., Wang, C., Yuhang, W., Xiao, S., and Yungui, C., 2018, “Effects of Hydrogen Content on Powder Metallurgy Characteristic of Titanium Hydrides,” *International Journal of Hydrogen Energy*, 43, pp. 7102–7107.
- [38] San-Martin, A. and Manchester, F.D., 1987, “The H-Ti (Hydrogen-Titanium) system,” *bulletin of Alloy Phase Diagrams*, **8**, pp. 30–42.
- [39] Paneth, F. and Hofeditz, W., 1929, “Ber Gesellschaft,” *Chemistry Europe*, **62**(5), pp. 1335–1347.
- [40] Paneth, F. and Lautsch, W., 1930, “Isolation of Radical Ethyl,” *Nature*, **125**, pp. 564.
- [41] Rice, F. and Glasebrook, A., 1934, “The Thermal Decomposition of Organic Compounds from the Standpoint of Free Radicals. XI. The Methylene Radical,” *J. Am. Chem. Soc.*, **56**(11), pp. 2381–2383.

- [42] Pearson, T.G., Purcell, R.H. and Saigh, G. S., 1938, "Methylene," J. Chem. Soc., **82**, 409.
- [43] Pearson, T.G., Robinson, P.L. and Stoddart, E.M., 1933, "The behavior of metals, particularly lead and bismuth, in atomic hydrogen, and attempts to prepare atomic hydrogen from hydrides," Proc. R. Soc. Lond., **142**, pp. 275–285.
- [44] Hiraoka, H., 1986, "Selective Removal of Metal Atoms in Hydrogen Reactive Ion Etching," J. of Vac. Sci. Tech B, **4**, pp. 345.
- [45] Chou, C. H. and Phillips, J., "Tin Foil Reconstruction in Hydrogen Plasma," J. Vac. Sci. and Techn. A, **8**, pp. 3941.
- [46] Wu, N.L. and Phillips, J., 1985, "Catalytic Etching of Platinum During Ethylene Oxidation," J. Phys. Chem., **89**(4), pp. 591–600.
- [47] Wu, N.L. and Phillips, J., 1986, "Reaction-Enhanced Sintering of Platinum Thin Films During Ethylene Oxidation," J. Appl. Phys., **59**, pp. 769.
- [48] Hess, J.M. and Phillips, J., 1992, "Catalytic Etching of Pt/Rh Gauzes," J. Catal., **136**, pp. 149.
- [49] Dean, V.W., Frenklach, M., Phillips, J., 1988, "Catalytic Etching of Platinum Foils and Thin Films in Hydrogen-Oxygen Mixtures," J. Phys. Chem., **92**(20), pp. 5731–5738.
- [50] Kaess, U., Majera, G., Stolla, M., Peterson, T. and Barnes, R.G., 1997, J. of Alloys and Comp., **259**, pp. 74.
- [51] Weigle, J.C. and Phillips, J., 2004, "Modeling Hydrogen Spillover in Dual-Bed Catalytic Reactors," AIChE J., **50**, pp. 821.
- [52] Weigle, J.C. and Phillips, J., 2004, "Novel Dual-Bed Reactors: Utilization of Hydrogen Spillover in Reactor Design," Langmuir, **20**(4), pp. 1189–93.
- [53] Chang, J., Phillips, J., and Heck, R., 1996, "Catalytic Synergism in Physical Mixtures," Langmuir, **12**(11), pp. 2756–2761.
- [54] Chang, H. and Phillips, J., 1977, "Catalytic Synergism in Physical Mixtures of Supported Iron-Cerium and Supported Noble Metal for Hydroisomerization of 1,3-Butadiene," Langmuir, **13**(3), pp. 477–482.
- [55] Menéndez, J.A., Radovic, L.R., Xia, B. and Phillips, J., 1996, "Low-Temperature Generation of Basic Carbon Surfaces by Hydrogen Spillover," J. Phys. Chem., **100**(43), pp. 17243-17248.

- [56] Evans, A.G., Hutchinson, J.W., Ashby, M.F., 1998, "Cellular metals," *Solid State and Material Science*, **3**, pp. 288–303.
- [57] Tuchinskiy, L., Loutfy, R., 2004, "Titanium Foams for Medical Applications," *Medical Device Materials*, pp. 377–381.
- [58] Zhao, C.Y., Kim, T., Lu, T. J. and Hodson, H. P., 2004, "Thermal Transport in High Porosity Cellular Metal Foams," *J. of Therm. and Heat Trans.*, **18**(3), pp. 309–317.
- [59] Banhart, J., 2001, "Manufacture, characterization and application of cellular metals and metal foams," *Progress in Mat. Sci.*, **46**, pp. 559–632.
- [60] Kashef, S., Asgari, A., Hilditch, T.B., Yan, W., Goel, V.K. and Hodgson, P. D., 2011, "Fatigue crack growth behavior of titanium foams for medical applications," *Mat. Sci. and Eng. A.*, **528**, pp. 1602–1607.
- [61] Kashef, S., Asgari, A., Hilditch, T.B., Yan, W., Goel, V.K., and Hodgson, P.D., 2010, "Fracture toughness of titanium foams for medical applications," *Mat. Sci. and Eng. A*, **527**, pp. 7689–7693.
- [62] Zhao, C.Y., Tassou, S.A. and Lu, T.J., 2008, "Analytical considerations of thermal radiation in cellular metal foams with open cells," *Int. J. of Heat and Mass Trans.*, **51**, pp. 929–940.

THIS PAGE INTENTIONALLY LEFT BLANK

INITIAL DISTRIBUTION LIST

1. Defense Technical Information Center
Ft. Belvoir, Virginia
2. Dudley Knox Library
Naval Postgraduate School
Monterey, California